APPLICATION OF FUNCTIONALIZED SUPERPARAMAGNETIC MESOPOROUS SILICATES

ADSORBENTS ON CLOFIBRIC ACID REMOVAL IN WASTEWATER

Miss Jidanan Kaosaiphun

A Thesis Submitted in Partial Fulfillment of the Requirements

for the Degree of Master of Science Program in Environmental Management

(Interdisciplinary Program)

Graduate School

Chulalongkorn University

Academic Year 2013

Copyright of Chulalongkorn University

การประยุกต์ใช้เมโซพอรัสซิลิเกตที่มีคุณสมบัติซุปเปอร์พาราแมกเนติกและต่อติดหมู่ฟังก์ชันในการกำจัดกรดคลอไฟบริคจากน้ำเสีย

นางสาวจิดานันท์ เกาสายพันธุ์

Thesis Title	APPLICATION OF FUNCTIONALIZED SUPERPARAMAGNETIC MESOPOROUS SILICATES ADSORBENTS ON CLOFIBRIC ACID REMOVAL IN WASTEWATER
By	Miss Jidanan Kaosaiphun
Field of Study	Environmental Management
Thesis Advisor	Assistant Professor Patiparn Punyapalakul, Ph.D.
Thesis Co-Advisor	Aunnop Wongrueng, Ph.D.

Accepted by the Graduate School, Chulalongkorn University in Partial Fulfillment of the Requirements for the Master's Degree

....Dean of the Graduate School

(Associate Professor Amon Petsom, Ph.D.)

THESIS COMMITTEE

....Chairman

(Assistant Professor Chantra Tongcumpou, Ph.D.)

....Thesis Advisor

(Assistant Professor Patiparn Punyapalakul, Ph.D.)

....Thesis Co-Advisor

(Aunnop Wongrueng, Ph.D.)

....Examiner

(Assistant Professor Chawalit Ngamcharussrivichai, Ph.D.)

....External Examiner

(Assistant Professor Suwanna Kitpatiboontanon, Ph.D.)

จิดานันท์ เกาสายพันธุ์ : การประยุกต์ใช้เมโซพอรัสซิลิเกตที่มีคุณสมบัติซุปเปอร์พาราแมก เนติกและต่อติดหมู่ฟังก์ชันในการกำจัดกรดคลอไฟบริคจากน้ำเสีย. (APPLICATION OF FUNCTIONALIZED SUPERPARAMAGNETIC MESOPOROUS SILICATES ADSORBENTS ON CLOFIBRIC ACID REMOVAL IN WASTEWATER) อ.ที่ปรึกษาวิทยานิพนธ์หลัก: ผศ. ดร. ปฏิภาณ ปัญญาพลกุล, อ.ที่ปรึกษาวิทยานิพนธ์ร่วม: อ. ดร. อรรณพ วงศ์เรือง, 106 หน้า.

งานวิจัยนี้มีจุดมุ่งหมายในการศึกษากลไกการดูดซับกรดคลอไฟบริคในช่วงความเข้มข้นสูง (mg/L) และความเข้มข้นต่ำ (µg/L) รวมทั้งผลกระทบของสารประกอบอินทรีย์ธรรมชาติที่มีความชอบ น้ำและไม่ชอบน้ำในน้ำเสียจริงต่อประสิทธิภาพการดูดซับ โดยใช้ตัวกลางดูดซับชนิดเมโซพอรัสซิลิเกตที่มี คุณสมบัติซูปเปอร์พาราแมกเนติกที่มีการติดต่อหมู่ฟังก์ชันต่างๆ (HMS-SPs) ได้แก่ หมู่ซิลานอล, หมู่อะมิ โน, และหมู่เมอแคบโต (HMS-SP 3N-HMS-SP และ M-HMS-SP ตามลำดับ) นอกจากนี้ยังได้ ทำการศึกษาประสิทธิภาพการคัดแยกตัวกลางดูดซับชนิด HMS-SP ออกจากน้ำโดยใช้ตัวกรองที่มีแรง แม่เหล็กเหนี่ยวนำ (High Gradient Magnetic Separation filter) ที่มีการดัดแปลงพื้นผิวเส้นใยสเตน เลสให้มีความไม่ชอบน้ำ โดยได้ศึกษาผลของอัตราการไหลของน้ำ และความเข้มข้นของตัวกลางดูดซับ

จลนพลศาสตร์การดูดซับกรดคลอไฟบริคเข้าสู่สมดุลในเวลา 6 ชั่วโมง และสอดคล้องกับ สมการปฏิกิริยาอันดับสองเสมือน ไอโซเทอมการดูดซับกรดคลอไฟบริคสอดคล้องกับสมการแบบฟรุนด์ ลิช จากผลการทดลองพบว่าที่ค่าพีเอช 5 HMS-SP ที่มีการติดต่อหมู่อะมิโน มีประสิทธิภาพการดูดซับ กรดคลอไฟบริคสูงสุดตามด้วยหมู่ซิลานอล และหมู่เมอร์แคบโตตามลำดับ โดยประสิทธิภาพการดูดซับ กรดคลอไฟบริคของตัวดูดซับที่มีการต่อติดกับหมู่ฟังก์ชัน มีสาเหตุมาจากแรงดึงดูดของพันธะไฮโดรเจน ระหว่างโมเลกุลของกรดคลอไฟบริคและหมู่ฟังก์ชันที่ทำการต่อติดบนพื้นผิวเป็นหลัก นอกจากนี้การมีอยู่ ของสารประกอบอินทรีย์ธรรมชาติที่มีความไม่ชอบน้ำนั้นทำให้ประสิทธิภาพในการดูดซับกรดคลอ ไฟบริคมีค่าลดลงน้อยกว่าในกรณีของสารประกอบอินทรีย์ธรรมชาติที่มีความชอบน้ำ ซึ่งเกี่ยวเนื่องกับ การแย่งชิงพื้นผิวตัวกลางดูดซับผ่านพันธะไฮโดรเจนเป็นหลัก

เวลาเบรคทรู (Breakthrough time) ของตัวกรองที่มีแรงแม่เหล็กเหนี่ยวนำ (HGMS filter) จะเพิ่มขึ้นจากการลดอัตราการไหลของน้ำ และลดความเข้มข้นของตัวกลางดูดซับ นอกจากนี้การ ปรับแต่งพื้นผิวเส้นใยสเตนเลส โดยการเพิ่มความไม่ชอบน้ำนั้นไม่ส่งผลต่อการกักเก็บตัวกลางดูดซับอย่าง มีนัยสำคัญ จากการทดลองสภาวะที่มีประสิทธิภาพสูงสุดคือ อัตราการไหลของน้ำมากกว่า 5 เมตรต่อ ชั่วโมงขึ้นไป และตัวกลางดูดซับที่มีความเข้มข้น 1 กรัมต่อลิตร

สาขาวิชา   การจัดการสิ่งแวดล้อม   ลายมือชื่อนิสิต ....

ปีการศึกษา 2556   ลายมือชื่อ อ.ที่ปรึกษาวิทยานิพนธ์หลัก ....

                                        ลายมือชื่อ อ.ที่ปรึกษาวิทยานิพนธ์ร่วม ....

5587657620 : MAJOR ENVIRONMENTAL MANAGEMENT

KEYWORDS: SUPERPARAMAGNETIC HEXAGONAL MESOPOROUS SILICATES / SURFACE FUNCTIONAL GROUPS / ADSORPTION / CLOFIBRIC ACID

JIDANAN KAOSAIPHUN: APPLICATION OF FUNCTIONALIZED SUPERPARAMAGNETIC MESOPOROUS SILICATES ADSORBENTS ON CLOFIBRIC ACID REMOVAL IN WASTEWATER. ADVISOR: ASST. PROF. PATIPARN PUNYAPALAKUL, Ph.D., CO-ADVISOR: AUNNOP WONGRUENG, Ph.D., 106 pp.

The objective of this research is to investigate clofibric acid (CFA) adsorption mechanism in high and low concentrations (mg/L and µg/L) and effects of hydrophobic and hydrophilic natural organic matter (NOM) fraction in real swine farm wastewater on functionalized superparamegnetic hexagonal mesoporous silicates (HMS-SPs). Three surface functional groups of synthesized HMS-SPs were applied in this study which is silanol, (ethoxysilylpropyl) diehtylenetriamine and 3-mercaptopropyltriethoxysilane group (HMS-SP, 3N-HMS-SP, and M-HMS-SP, respectively). Furthermore, separation efficiency of adsorbent by modified hydrophobicity surface of High Gradient Magnetic Separation filter (HGMS filter) at various flow rate and particle concentration was also investigated.

The CFA adsorption reached the equilibrium at 6 hrs and adsorption kinetic and isotherms were well fitted with pseudo-second-order model and Freundlich model, respectively. At pH 5, 3N-HMS-SP had highest CFA adsorption rate and capacity following with HMS-SP and M-HMS-SP respectively. Adsorption of CFA on all surface functional groups was strongly related to hydrogen bonding between CFA and surface functional groups. Furthermore, the hydrophobic NOM fraction had lower effect on CFA adsorption than the hydrophilic NOM fraction by decreasing adsorption capacities due to active surface competition via hydrogen bonding.

The breakthrough times of HGMS filter were enhanced by decreasing of flow rate, and particle concentration. However, hydrophobic modified stainless fiber could not enhance the retention of HMS-SP particle, significantly. The highest separation capacity on this research was conducted in flow rate higher than 5 m/hr and 1 g/L of particle concentration.

Field of Study: Environmental Management   Student's Signature ....

Academic Year: 2013   Advisor's Signature ....

Co-Advisor's Signature ....

ACKNOWLEDGEMENTS

CONTENTS

LIST OF FIGURES

LIST OF TABLES

CHAPTER I

INTRODUCTION

1.1 State of Problems

Pharmaceutical and personal care products (PPCPs), pharmaceutical active compounds (PhACs) are widely used for treatment, livestock and agriculture due to pharmaceutical compounds can use in humans, animals and plants (Zuccato, 2000). Whereas, many pharmaceutical compounds cannot eliminated completely by metabolism of humans and animals, hence their residue compounds can disperse to environment via excreta and can contaminate in soil, groundwater, and surface water. Therefore, pharmaceutical residue compounds have become the important problem of environment. Several researches reported that the concentration of pharmaceutical residue compounds can be detected in surface water and groundwater up to µg/L (Kummerer, 2009; Reddersen, 2002; Skadsen, 2004).

Recently, pharmaceutical residues can be treated by several methods for example; using nanofiltration/reverse osmosis (NF/RO) membranes (UTC-60 and LF10) to remove six pharmaceutical residues compound (Clofibric acid, Diclofenac, Ketoprofen, Mefenamic acid, Carbamazepine, and Primidone). Those (NF/RO) membranes process was used as the supplementary process of conventional activated sludge process followed by media filtration (i.e., tertiary treatment). Moreover, treatment with a membrane bioreactor (MBR)) was investigated and reported the percent of rejection in six pharmaceutical residues at approximately > 95% depend on the type of wastewater treatment (Kimura, 2009). Ozonation was studied as a pre-treatment process for eliminated of anti-inflammatory residuals; that

reported the conversion percentage at 90% for Diclofenac-Na (DCF) and just only 26% and 46% of mineralization by hybrid ozonation which is O_3/UV/US and O_3/US/Fe^{2+}, respectively (Ziylan, 2013). Modified chitosan adsorbents that cross-linked with glutaraldehyde and grafted with sulfonate (CsSLF) or N-(2-carboxybenzyl) groups (CsNCB) were investigated the removal efficiencies of pharmaceutical contaminants (pramipexole dihydrochloride) from wastewaters. It was found that removal efficiency by using CsSLF and CsNCB was 95% and 94%, respectively (Kyzas, 2013).

Consequently, Adsorption process, as a simple and low cost method, is widely used in the removal of persistent organic micro-pollutants. Many researchers studied the adsorption process for removal pharmaceutical residues from wastewater. For example, effects of drug concentration on adsorption of Levofloxacin by polyacrylonitrile (PAN) haemofilters were studied and suggested that adsorption by haemofilters in vitro was unlikely to affect Levofloxacin pharmacokinetics significantly in vivo (G. Tian, Gomersall, C. D., Wong, A., Leung, P., Choi, G., Joynt, G. M., Tan, P. and Lipmana, J. , 2006). Using modified sugarcane bagasse (SB) as an adsorbent can remove Levofloxacin around 37% from acidic solution (in vitro); adsorption capacity was 0.152 mg/g at 2 ppm, which increased up to 0.42 mg/g at 10 ppm (Khan, 2011). Hence, adsorption process with modified adsorbents would be the interesting process for removal of pharmaceutical residue compounds from wastewater.

The pharmaceutical active compounds (PhACs) and their metabolites in aquatic systems has become a concern in the recent years due to their generally persistent and omnipresence in the environment. Clofibric acid (CFA) is one of the most reports to eco-toxicological impact in wastewater due to this compound effect to microbial

communities and animal. For instance, CFA can effect to a reproductive toxicity on daphnia with a LOEC (lowest observed effect concentration) of 10 µg/L (Ferrari, 2003). This CFA can metabolite in water resource and the pathway is shown in **Figure 1.1**.
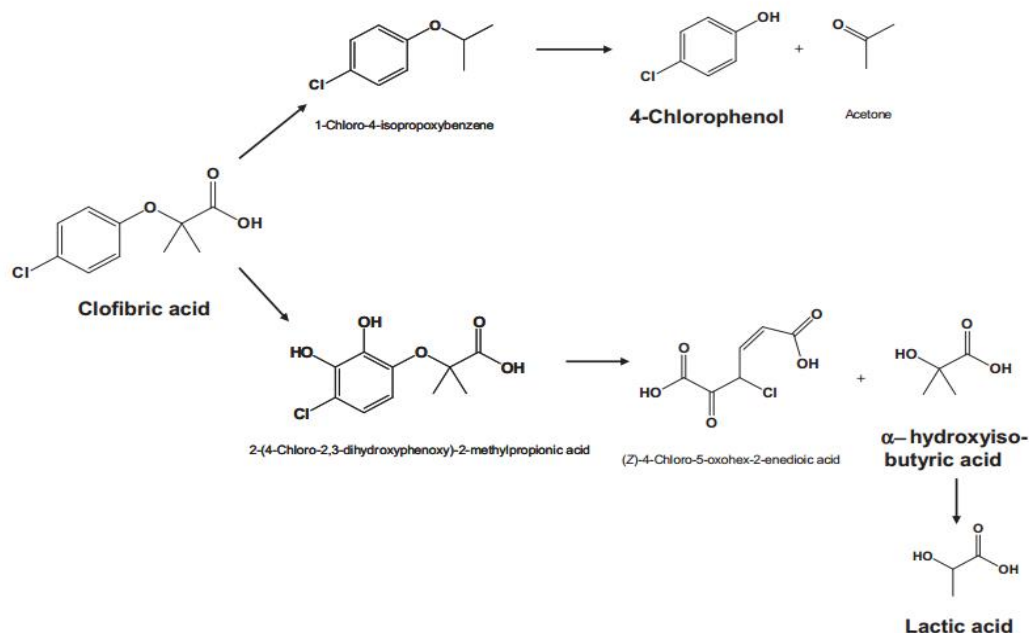
Figure 1. 1 Parent and metabolites compounds of Clofibric acid (Salgado, 2012)

One metabolite compound of CFA is Lactic acid that can cause many effects to human and animal in acute and chronic toxicity such as system of dermal, inhalation, oral routes, and endocrine (US.EPA, 2009). Moreover, another one metabolites compound is 4-chlorophenol or *p*-chlorophenol is a toxic compound and can be used as an intermediate for the synthesis of insecticides, herbicides, and preservative that effect to oral routes. Hence, this study will focus on removal of Clofibric acid from synthetic wastewater which has the co-existing compound as same as in real wastewater.

Mesoporous silicas are widely used to adsorb micro-pollutant due to their large surface area and uniform pore size that can improve adsorption capacity and selectivity for target pollutants by functionalization of oganosilane functional group. Moreover, efficiency of adsorbent separation from wastewater can be enhanced by adding the superparamagnetic property into the adsorbent particles. Hexagonal mesoporous silicates (HMSs) are suitable mesoporous silica for using in this research because it has pore size between 2 nm and 50 nm which might enhance the intraparticle diffusion of CFA, which has molecule size at 0.94 nm (Nie, 2013). Furthermore, HMS can be improved the ability of separation by modifying with the magnetite nanoparticle (Fe_3O_4) which made from Iron (II) and Iron (III). The magnetite nanoparticle (Fe_3O_4) is coated with HMS porous structure which can be called as superparamagnetic hexagonal mesoporous silicates (HMS-SP). Hence, the HMS-SP is supposed to be the pristine adsorbent which can be functionalized but also can be separated effectively by low energy magnetic field unit operation.

High Gradient Magnetic Separation Filter (HGMS filter) is generally used to separate magnetic materials from non-magnetic solution by using magnetic filtration to hold the magnetic particles in magnetic filter media, for instance, wire stainless which influenced on the magnetic field from permanent magnet and modification of wire stainless to increase hydrophobicity in surface in order to enhance the capacity of adsorbent separation. Hence, in this study, HGMS filter are selected to be the unit separation model for removal synthesized HMS-SPs after adsorption process is finished.

The aims of this research are to investigate the effect of surface functional group on Clofibric acid (CFA) adsorption capacity by using HMS-SPs as the adsorbents and to determine the flow rate and particle concentration condition that suitable for separating HMS-SP by HGMS filter.

1.2 Objectives

1.2.1 To investigate adsorption efficiencies for Clofibric acid (CFA) removal by using surface functionalized superparamagnetic mesoporous silicates.

1.2.1.1 To determine the effect of pH on CFA adsorption capacities and adsorption mechanisms of hydrophobic and hydrophilic surface functional groups at high concentration.

1.2.1.2 To investigate the CFA adsorption capacity at low concentration.

1.2.1.3 To identify the effects of hydrophobic and hydrophilic natural organic matters (NOMs) in real wastewater on CFA adsorption capacities.

1.2.2 To investigate the effect of flow rate and particle concentration on separation of superparamagnetic mesoporous silicates from synthetic wastewater by hydrophobic modified High Gradient Magnetic Separation Filter (HGMS filter)

1.3 Hypotheses

1.3.1 Modification of hydrophilic functional group on adsorbent surface might enhance the CFA adsorption capacity.

1.3.2 The adsorption mechanism depends on hydrogen bonding, hydrophobic interaction, and electrostatic interaction.

1.3.3 Hydrophobic and hydrophilic natural organic matters (NOM) in real wastewater might effect to CFA adsorption capacities due to active site competition.

1.3.4 Hydrophobic wire stainless of High Gradient Magnetic Separation Filter (HGMS filter) can enhance separation of the superparamagnetic particle.

1.3.5 Lower flow rate in High Gradient Magnetic Separation Filter (HGMS filter) should has higher separation efficiency.

1.4 Scopes of the Study

This research was conducted at Department of Environmental Engineering, Faculty of Engineering and NCE-EHWM laboratory, Chulalongkorn University. There are six parts of this study which consist of;

1.4.1 <u>Synthesis of adsorbents</u>

Adsorbents which were used in this study are superparamagnetic mesoporous silicates, functionalized superparamagnetic mesoporous silicates consist of 3-aminopropyltriethoxysiliane and 3-mercaptopropyltriethoxysilane. Adsorption information was compared with commercial powdered activated carbon (PAC).

1.4.2 <u>Characterization of adsorbents</u>

Characterization of physiochemical properties of synthesized adsorbents were analyzed, such as surface charge, elemental analysis, BET surface area, crystal structure (XRD pattern), particle size, and FTIR pattern.

1.4.3   Adsorption study of Clofibric acid (CFA) on adsorbents at high concentration

Clofibric acid (CFA) adsorptions were conducted at high concentration (0-15 mg/L) of synthesis wastewater to determine the adsorption kinetic, adsorption mechanism, adsorption capacity, and effect of pH (5, 7, 9) on adsorption capacity.

1.4.4   Adsorption study of Clofibric acid (CFA) on adsorbents at low concentration

Clofibric acid (CFA) adsorption isotherm of the most appropriate adsorbent from 1.4.3 at low concentration (50-200 μg/L) was determined by using synthesis wastewater.

1.4.5   Adsorption study of Clofibric acid (CFA) on adsorbent with real wastewater

Clofibric acid (CFA) adsorptions were conducted under high concentration (0-15 mg/L) by using real wastewater from swine farm in northern part of Thailand. NOMs in collected wastewater were separated to be hydrophobic and hydrophilic NOM and were studied the effect on adsorption capacity.

1.4.6   Separation of adsorbents

High Gradient Magnetic Separation Filtration (HGMS filter) was used to separate adsorbents from synthesis wastewater by varying the concentration of adsorbents (0.3, 0.6, 1 g/L), flow rate of filtration (3, 5, 7 m/hr). Moreover, surface of stainless wire in HGMS filter was modified by dripping silica sol-gel solution in order to coat hydrophobic functional group.

The scopes of this study are as followed in 6 parts and the experimental framework shows in **Figure 1.2**;
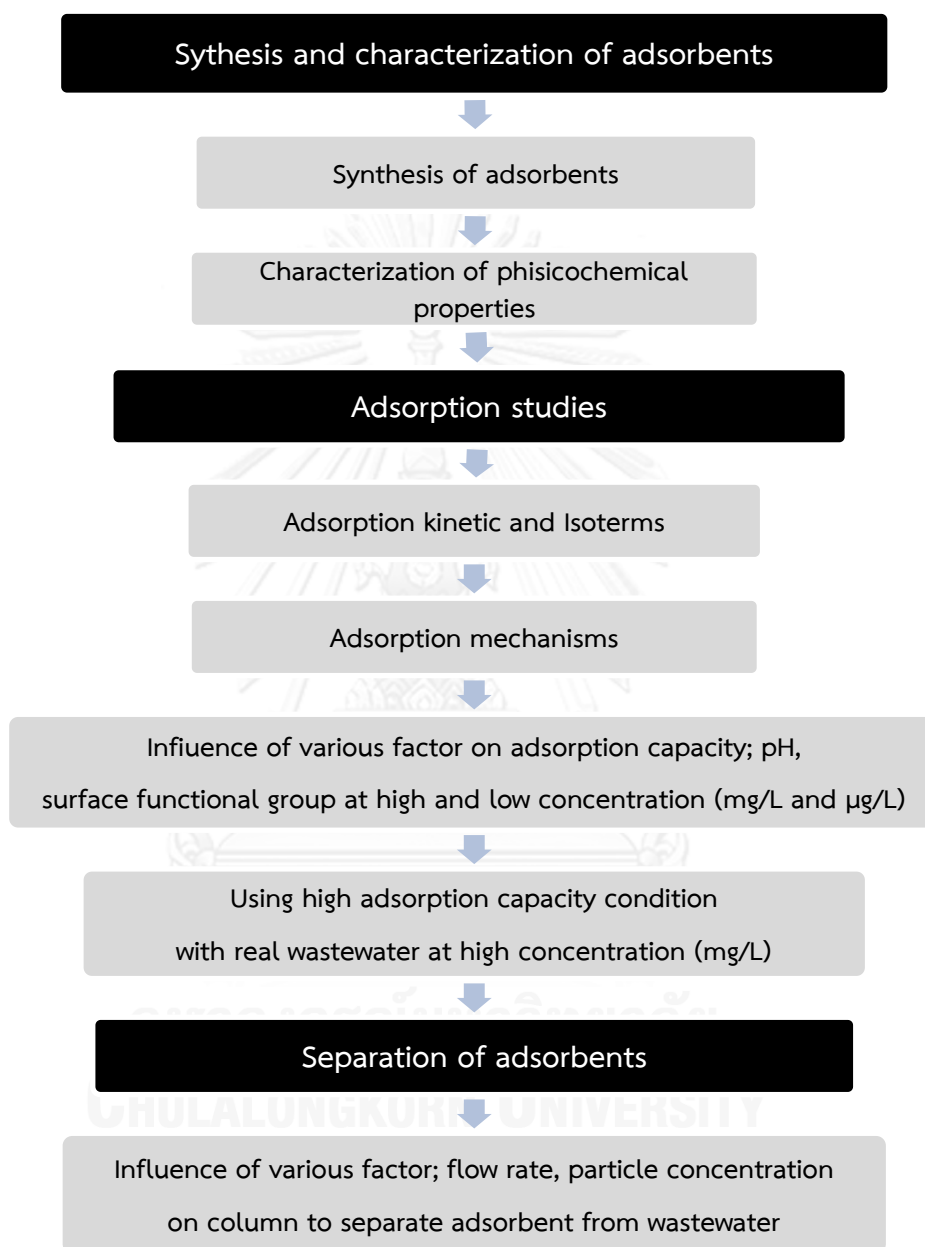
Figure 1. 2 Experimental framework of this study

CHAPTER II

THEORETICAL BACKGROUNDS AND LITERATURE REVIEWS

2.1 Pharmaceuticals in the environment

Pharmaceutical and personal care products (PPCPs), pharmaceutical active compounds (PhACs) are widely used for treatment, livestock and agriculture due to pharmaceutical compounds can use in humans, animals and plants (Zuccato, 2000). Whereas, many pharmaceutical compounds are not eliminated completely in humans and animals, their residue compounds disperse to environment that shows in **Figure 2.1** (Mompelat, 2009).
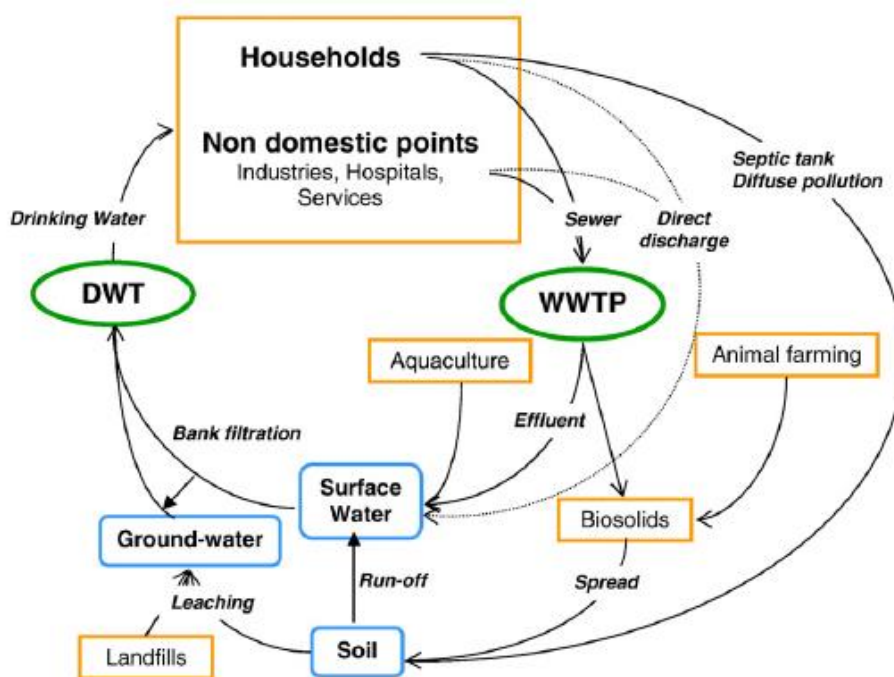
Figure 2. 1 Origin of pharmaceutical residue compounds

The contaminate in soil from many researches can be analyzed in 23% of soil sample found that can detected chlortetracycline (CTC) in soil samples (Martı́nez-Carballo, 2007), residual concentrations of antibiotics were estimated for agricultural soil, ranging for tetracyclines (TCs) from 450 to 900 µg/kg, for macrolides from 13 to

67 µg/kg and for fluoroquinolones (FQs) from 6 to 52 µg/kg. While, the pharmaceutical residual contaminant in groundwater and surface water such as Guanylurea was detected in sewage treatment plants (STP) effluents and surface waters at concentrations of 39–56 µg/L and 1.8–3.9 µg/L, respectively (Oosterhuis, 2013). Codeine was detected in groundwater sites from the united states of America at concentration of 0.24 µg/L (Barnes, 2008). Those pollutants have many effects to ecosystem such as decreasing of fish reproduction, change embryo of cattle (Brandhof, 2010).

2.2 Clofibric acid (CFA)

Clofibric acid is the main active derivative substance of Clofibrate and several other fibrates, evolved to enhance lipid metabolism in human (lipid lowering agent) that used widespread. It can distribute to environment and persist for long periods, since it is non-biodegradable (Nunes, 2008). **Table 2.1** demonstrates general properties of Clofibric acid and **Figure 2.2** shows the structure of Clofibric acid.

Table 2. 1 General properties of Clofibric acid (CFA)

Parameters	Descriptions
Molecular weight	214.6 g/mol [a]
Melting point	118-123 °C [a]
Solubility in water	582.5 mg/L [a]
pK_a	3.81 [b]
Log K_{ow}	2.57 [c]
Formula	$C_{10}H_{11}ClO_3$ [a]

a: http://en.wikipedia.org/wiki/Clofibric_acid (accessed on 3 Nov 2013) b: Loffler et al.,2005 c: Tixier et al.,2003
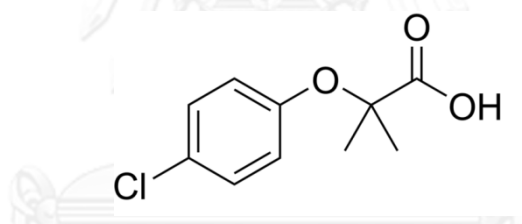
Figure 2. 2 The structure of Clofibric acid

2.3 Occurrence of CFA in environment

The aquatic environment receives inputs of many compounds from agricultural, livestock, industrial, and other activities of human. Pesticides are the main contamination for water resources because they are always used directly to soil and can be leached into groundwater and surface water. Therefore, pesticides have been detected in aquatic environment especially the group of phenoxyalkanoic acid. Clofibric acid (CFA, a pharmaceutical drug) is also one of phenoxyalkanoic acid group and a structure isomer of CFA is propionic acid (a herbicide). CFA has high volume production because it is mainly used in form of clofibrate in personal medical care as

a blood lipid regulator by using in patients for long time. CFA appears in metabolize form and more stable than the other related compounds (Buser, 1998). In the recent years, CFA has been found in variety of concentrations and places; 1.6 µg/L in the majority of sewage treatment plants (Ternes, 1998), 0.55 µg/L in surface waters of Swiss lakes (Buser, 1998), 270 ng/L in tap water (Heberer, 2002), and 103 ng/L in Detroit River water (Boyd, 2003). It has eco-toxicity such as effect to microbial communities and animal especially daphnia in lowest concentration at 10 µg/L. Hence, the source of CFA contamination is not just only the agricultural activities but also the residue of used pharmaceutical products and their pathway metabolites.

2.4 Current treatment technology for CFA

Previous studies reported several CFA treatment methods. For example, biodegradation method by using Sequential Batch Reactor (SBR) was studied by adding CFA and propanil to facilitate biomass growth and potentially co-metabolism. The process was operated for long cycle until 12 months, and CFA removal can be estimated at 51% of initial CFA concentration at 6 mg/L (Salgado, 2012). Ozonation method was compared by using catalytic and non-catalytic ozonation to degrade the aqueous solution of CFA. The ozonation with the presence of TiO_2 as catalyst can enhance the CFA degradation and CFA can be removed completely after15 min at pH5 (Rosal, 2009). Biosorption method by using agricultural waste rice straw to adsorbed CFA in aqueous solution was also reported. The highest CFA adsorption at 42.5% was obtained at rice straw biosorbent (RSB) dosage of 30 g/L, while the pH was about 3.1 (Liu, 2013).

2.5 Adsorption

Adsorption process involves separation of a substance or adsorbate from one phase, followed by its accumulation onto the surface of the adsorbing phase or adsorbent (Gökmen, 2002). The sorption ability of different sorbents is strongly dependent on the available surface area, polarity, contact time, pH and the degree of hydrophobic nature of the adsorbent and adsorbate (Nadeema, 2006).

Fundamental

Adsorption mechanism consists of three steps (Yousef, 2011). The first step is adsorbate transports to external surface of adsorbent that call film diffusion process. The second step is adsorbate moves to inter part of adsorbent that call pore diffusion process. Finally, the third step is adsorbate adsorbs to internal surface of adsorbent pore that call adsorption process. Normally, the third step is assumed to be faster than others and the slowest step is rate limiting step of adsorption process.

Theory of adsorption

Capacity

The adsorption capacity of adsorbent can be determined from mass balance equation as shown in equation (2.1);

$$q = \frac{(c_0 - c_e)}{M} \times V \qquad (2.1)$$

Where C_0 and C_e is the initial and the equilibrium concentration of the adsorbate (mg/L) respectively, q is the adsorption capacity (mg/g), M is the mass of adsorbent (g) and V is the volume of solution (L).

Kinetic

The adsorption kinetic is used to predict and design adsorption systems. While chemical kinetics describes the rate of chemical reaction and the affecting of factors from the reaction rate. Measurement of sorption rate constants can be done by evaluating the basic quantities of sorbent such as the time required for a sorbent to remove particular compounds (Mall, 2006).

-   The pseudo-first order kinetic model can be determined from equation (2.2);

$$\frac{1}{q} = \frac{k_1}{q_e t} + \frac{1}{q_e} \tag{2.2}$$

Where q_t is the amount of adsorbed (mg/g) at time t (min), q_e is the amount of adsorbed (mg/g) at equilibrium and k_1 is the pseudo-first order rate (mg/g). The values of k_1 and q_e are calculated from slope and intercept of the plots between 1/q and 1/t.

-   The pseudo-second order kinetic model can be determined from equation (2.3);

$$\frac{t}{q_t} = \frac{1}{k_2 q_e^2} + \frac{t}{q_e} \tag{2.3}$$

Where k_2 is the pseudo-second order rate constant is calculated from the plots between t/q_t and t (Abdullah, 2009). According to the pseudo-second-order model, the initial adsorption rate (*h*) (mg/g. h) can be determined according to Equation (2.4);

$$h = K_2 qe^2 \tag{2.4}$$

Isotherm

Adsorption isotherm shows the relationship between adsorption capacity of the adsorbent and equilibrium concentration of adsorbate, which is the critical importance information for optimizing the use of the adsorbents (Ho, 2005). The isotherms which will be applied in this research consist of three mathematic isotherm models;

- **Langmuir isotherm**

  The Langmuir isotherm of linear form is calculated according to the following equation (2.5);

  $$\frac{1}{q_e} = \frac{1}{q_m} + \frac{1}{k_L q_m C_e} \qquad (2.5)$$

  Where k_L is the Langmuir constant (L.mg^{-1}) and q_m is the maximum adsorption capacity (mg/g). The dimensionless separation factor R_L is use to predict desirability of adsorption according to the following equation (2.6);

  $$R_L = \frac{1}{1+K_L C_0} \qquad (2.6)$$

  Where C_0 is the initial concentration of pharmaceuticals (µg/L).

- **Freundlich isotherm**

  The Freundlich isotherm in linear form is shown in following equation (2.7);

  $$\ln q_e = \ln k_F + \frac{1}{n} \ln C_e \qquad (2.7)$$

  Where k_F is the Freundlich constant and n is the adsorption intensity (dimensionless).

- **Linear isotherm**

The linear isotherm calculated according to the following equation (2.8);

$$q_e = K_p C_e \qquad (2.8)$$

Where K_p is the linear constant (L/g) (Samuel, 1987).

2.6 Mesoporous Silicate

The first discovery of ordered mesoporous silicates since 1992 by Mobil scientists (Tanev, 1994), these materials are interested attention due to high surface areas, large pore volumes, uniform pore size in the range of 2-30 nm, and tunable surface functional groups. The particularity features of mesoporous materials that suitable for many applications such as catalysis, separation, and adsorption (H. Tian, Li, J., Shen, Q., Wang, H., Hao, Z., Zou, L. and Hu, Q., 2009; Wang, 2008).

There are three kinds of the mesoporous material synthesis procedures consist of; Firstly, M41S feature of silica and aluminosilicates (such as hexagonal MCM-41, cubic MCM-48 and lamellar MCM-50) synthesized by charge matching between ionic surfactants and ionic inorganic reagents. Secondly, the mesoporous materials synthesized by using two neutral routes based on self-assembly and hydrogen bonding, which one is hexagonal material (HMS and MSU) and the advantage is it can remove the organic phase by solvent extraction (Tanev, 1994). Finally, the group of mesoporous materials is involving amphiphilic di- and tri-block copolymers as the organic structure directing agents (SBA15). The advantages of this material are large monodispersed mesoporous (up to 50 nm) and thicker walls (Zhao D., 1998).

Synthesis of Hexagonal Mesoporous Silicates (HMS)

The neutral template route (S0I0) was used to synthesis HMS by based on hydrogen bonding and self-assembly between neutral primary amine micelles (S0) and neutral inorganic precursors (I0). Further, removal of HMS template method was completed by solvent extraction or calcination in air (Lin, 2005; Pinnavaia, 1995).

Adsorbent surface modification

There are two fundamental approaches consist of the post synthetic functionalization of silica or post grafting method and the co-condensation method, for the synthesis of the functionalized silica process.

- Post synthetic functionalization of silicas or post grafting method

Post grafting method, the functional groups were attached onto pore surface of mesoporous silicate. The advantage of grafting is it could maintain the mesostructure after modifying. Moreover, this method is hard to control the dissemination and concentration of functional group that shown in **Figure 2.3** (Stein, 2000). Then, silylation is commonly functionalized surface with organic groups as following procedure:

$$\equiv Si\text{-}OH + Cl\text{-}SiR_3 \xrightarrow{\phantom{100\,^{\circ}C}} \equiv Si\text{-}OSiR_3 + HCl$$

$$\equiv Si\text{-}OH + R'O\text{-}SiR_3 \xrightarrow{100\,^{\circ}C} \equiv Si\text{-}OSiR_3 + HOR'$$

$$2\equiv Si\text{-}OH + HN(SiR_3)_2 \xrightarrow{25\,^{\circ}C} 2\equiv Si\text{-}OSiR_3 + NH_3$$
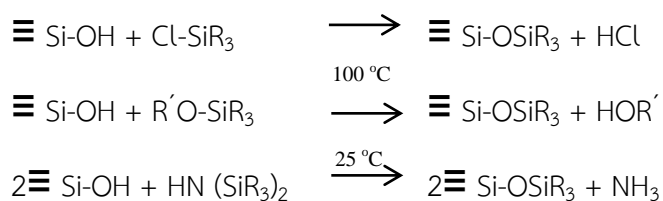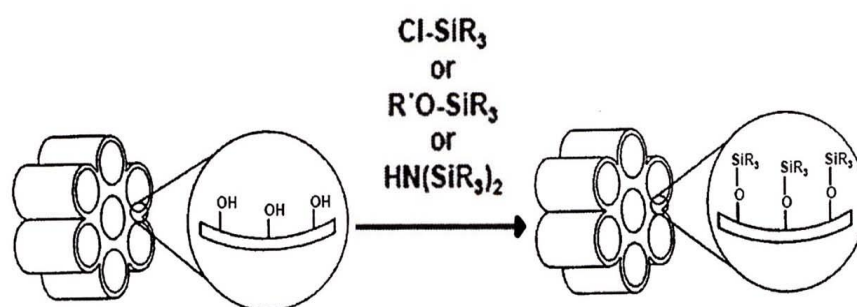
Figure 2. 3 Functioanlization of mesoporous silicates by post grafting

- Co-condensation method

Co-condensation method, the functional groups were condensation with tetraethoxysilane or terminal trialkoxyorganosilanes (TEOS or TMOS) while synthesized template. The advantage of this method is higher loading functional groups. However, it could loss original structure after modifying that shown in **Figure 2.4** (Hoffmann, 2006). The comparison between grafting and co-condensation methods is summarized in **Table 2.2** (Maria, 2004).

Figure 2. 4 Co-condensation method for the organic modification of mesoporous pure silica phases, R= organic functional group

Table 2. 2 Advantage and disadvantage of two surface modification methods

	Post grafting method	Co-condensation method
Advantage	• Good preservation of the mesostructure after post-grafting	• Higher and more uniform surface coverage of functionality • Capable control in surface properties
Disadvantage	• Reduce pore size and pore volume • Limited loading level of the functional groups can be grafted because of the limited density of the reactive surface silanols • Time consuming • Ineffective due to partial cross-linking of the functional groups with the silica-surface silanol groups • Obtain low density and non-uniformity of functionality	• Loss in original structure ordering such as aminopropyltriethoxysilane (APTES) functionalization • Poor control of functional group on the surface

Mesoporous silicas are widely use in adsorption field and suitable for modify the separation property by adding superparamagnetic characteristic into the core of mesoporous particle. Therefore, this study will select the superparamagnetic mesoporous silicates to study their application for CFA adsorption and related unit operation process.

2.7 High Gradient Magnetic Separation Filter

Recently, High Gradient Magnetic Separation Filter (HGMS filter) is normally to use in magnetic filtration that separate magnetic materials from non-magnetic solution. The methods to generate external magnetic field consist of three ways; permanent magnet (Sato, 2004), electromagnetic solenoid (Ditsch, 2005), and

superconducting magnet (Baik, 2010; Misuhashi, 2003). The mechanism of magnetic filtration is to enhance the attachment between magnetic particles and the magnetic filter media that set by stainless steel. This separation process is low cost and easy to operate.

Due to the HGMS filter has competency to separate magnetic material from non-material solution. Therefore, the HGMS might be suitable for removal HMS-SPs particles, which has magnetic property. This research plans to investigate the operation condition of HGMS filtration by varying concentration of adsorbents and flow rate of filtration.

Theory of Magnetic Separation

- **Magnetic strength field (H)**

The magnetic strength field is the quantity of magnetizing force that created to magnetic material by magnetic current.

- **Magnetic flux density (B)**

The magnetic flux density is the amount of internal of magnetizing force that magnetic materials for instant permanent magnet give the magnetic force. Magnetic flux density depends on the magnetic permeability of material and magnetic strength field can be determined from equation (2.9);

$$B = \mu_m.H \qquad (2.9)$$

Where H is magnetic strength field (A.M^{-1}), B is magnetic flux density (T or Wb/m), and μ_m is magnetic permeability of material (Wb/(A.m)).

- **Magnetic force**

The magnetic force is the force of moving charge that determines in the Lorentz Law; according to following in equation (2.10);

$$F_m = q \, (v \times B) \qquad (2.10)$$

Where F_m is magnetic force (N), q is the electric charge of the particle (C), v is the instantaneous velocity of the particle (m.s^{-1}), and B is the magnetic field (T).

Then, magnetic force of particle when applies the magnetic field is shown in equation (2.11);

$$F_m = \mu_0 V_p M_p \cdot \nabla H \qquad (2.11)$$

Where F_m is magnetic force of particle, μ_0 is magnetic permeability of vacuum (Wb/(A.m)), V_p is particle volume (m^3), M_p is the particle magnetization (A/m), and ∇H is the gradient of magnetic strength field at the position of the particle.

There are three forces that involved in magnetic filtration process consist of;

- **Gravitational force**

The gravitational force is the force that drags the particles to fall down in the fluid by their own weight due to gravity; it can be determined from equation (2.12);

$$F_g = (\rho_p - \rho_g)V_p \qquad (2.12)$$

Where F_g is gravitation force (N), ρ_p is density of particle (kg/m), ρ_g is density of fluid (kg/m), and V_p is gravitational acceleration (m/s).

- **Centrifugal force**

The centrifugal force is the movement force that occurs when the particle is agitated, according to following in equation (2.13);

$$F_c = (\rho_p - \rho_g)\omega V_p r \quad (2.13)$$

Where F_c is centrifugal force (N), ω is the angular velocity (rad/s), and r is the radial of the particle (m).

- **Drag force**

The drag force is the frictional force of particle reaction to gravity force, now known as Stoke's law. F_d is drag force, which is calculated by equation (2.14);

$$F_d = 3\pi\eta d_p(v_f - v_p) \quad (2.14)$$

Where η is the dynamic viscosity of fluid (N.s/m^2), and d_p is the diameter of the particle (m).

2.8 Natural Organic Matters (NOMs)

Natural Organic Matters (NOMs) are a complex mixture with various chemical compositions and molecular size that occurs in natural water and originates from living and dead of plants, animals, and microorganisms. NOMs consist of hydrophilic and hydrophobic components (Matilainen, 2011). Moreover, NOMs can cause various problems in adsorption process in real wastewater treatment, since it may interact with target compounds or adsorbate that means decreasing of adsorption capacity of target compound. Moreover, competition between NOMs and target adsorbate to be adsorbed by adsorbent surface have to be considered, in case of NOMs can hold with adsorbent surface, it mean that selectivity of adsorbent might be changed and caused the reduction of target adsorption capacity.

2.9 Literature reviews

    2.9.1   Removal of pharmaceutical

(Bui, 2009) investigated that mesoporous silicate SBA-15 can remove the pharmaceutical such as carbamazepine, clofibric acid, diclofenac, ibuprofen, and ketoprofen from synthetic wastewater by adsorption capacity of all pharmaceuticals were high except clofibric acid. All adsorption kinetics and isotherms were fitted with pseudo second order model and Freundlich model. The interaction of mechanisms were controlled by hydrophilic interaction.

(Cabrera-Lafaurie, 2012) studied the adsorption of salicylic acid, clofibric acid, carbamazepine, and caffeine from synthetic wastewater by modified inorganic-organic pillared clays (IOCs) with Co^{2+}, Cu^{2+}, and Ni^{2+}. This research suggested that complexation between adsorbents and adsorbates were depended on ambient condition and it may be reversible interaction force at low concentration. According to the results, Ni^{2+} IOCs had the highest adsorption with salicylic acid and clofibric acid, while Co^{2+} IOCs had the greatest caffeine adsorption at low concentration. On the other side, all of modified IOCs had low adsorption capacity of carbamazepine due to the lack of surface functional groups to interact with adsorbate.

(Punyapalakul, 2004) investigated adsorption mechanism of pharmaceuticals; diclofenac and carbamazepine on functionalized hexagonal mesoporous silicates (HMS) instance amino and mercapto groups were performed by co-condensation method compare with SBA-15 and MCM-41 plus powdered activated carbon. The adsorption kinetics and isotherms were match with pseudo second order and linear models, respectively. The mercapto group on HMS had highest adsorption capacity in

order to enhancing of hydrogen bonding and hydrophobic interaction and the adsorption capacity of each adsorbent related to molecule size and effect of pH.

(Punyapalakul, 2004) investigated effect of functional groups of HMS on dichloroacetic acid (DCAA) adsorption comparison of three surface functional groups; amino, mercapto, and akyl groups. This research indicated that the amino group adsorbed DCAA by hydrophobicity interaction and adsorption capacity of mercapto and amino groups can increase due to active surface size were high.

(Bui, 2010) reported that effect of pharmaceutical adsorption; carbamazepine, diclofenac, ketoprofen, and ibuprofen by varied ionic strengths, different anions, divalent cations (Ca^{2+} and Mg^{2+}), trivalent (Al^{3+} and Fe^{3+}), and natural organic matter (NOM) on porous silica. This experiments were controlled high ionic strength by the ketoprofen adsorption capacity was increased while carbamazepine adsorption was decreased. Trivalent metal cations were increased in three acidic pharmaceuticals adsorption due to inner-sphere complex with surface and aqueous metal species. Divalent cations were enhanced the ibuprofen and ketoprofen adsorption at low concentration. Whereas, all pharmaceutical adsorptions were reduced by NOM, except for diclofenac adsorption. Therefore, the ionic strength, divalent and trivalent cations, and NOM are important factors to study in effect of adsorption.

2.9.2 Application of high gradient magnetic separation filter

Several researches which studies new technique to separation mesoporous silicate by coated magnetic material, that has magnetic properties and apply to use with high gradient magnetic separation (HGMS) filtration.

(Hua, 2003) studies application of high gradient magnetic separation by synthesized hexagonal mesoporous silicate (HMS) and encapsulated HMS with magnetic material, which called HMS-SP that used to adsorb DDT in water and separation from aqueous phase by magnet force. This research reported that DDT adsorption capacity was high on HMS-SP and significant effective with magnetic separation.

(Ruangtrakul, 2010) investigated that modified surface functional groups of HMS-SP had high adsorption of Naproxen (NAX) and applied magnetics separation to use in this experiments by HGMS filter. As the results of this study, the functionalized of HMS-SPs were selective to adsorb the NAX and removal of NAX from synthetic wastewater. Moreover, HGMS filter had efficiency of the HMS-SP separation from synthetic wastewater that using permanent magnets.

(Lortragool, 2009) studied the treatment of oily wastewater by using fibrous stainless steel as a coalescing medium to improve the treatment efficiency by modification of hydrophobicity on stainless steel surface. This study indicated that the efficiency to treatment oil from wastewater was enhanced for modified stainless steel surface.

Therefore, this research was investigated CFA adsorption both high concentration and low concentration and effect of natural organic matter (NOM) to efficiency of CFA adsorption. Moreover, this research was conducted the separation

of adsorbent by high gradient magnetic separation filter which modification hydrophobic surface of wire stainless filter.

CHAPTER III

MATERIALS AND METHODS

3.1 Materials

3.1.1 Pharmaceutical residue

- Clofibric acid 97% was purchased from Aldrich.

3.1.2 Synthesis of adsorbents

- **Superparamagnetic iron oxide particles (SP)**

  - Ammonium hydroxide 25% from J. T. Baker.

  - Iron (II) chloridetetrahydratewas purchased from Fluka.

  - Iron (III) chloridehexahydratewaspurchasedfromAjax Finechem.

  - Oleic acid was purchased from CrloErba.

- **Superparamagnetic hexagonal mesoporous silicate (HMS-SP)**

  - Acetone was purchased from Lab Scan.

  - Dodecylamine 98% was purchased from Acros organics

  - Hydrochloric 37% was purchased from CrloErba.

  - Tetraethoxysilan reagent grade 98% was purchased from Aldrich.

3.1.3 Organic functional groups

- 3-aminopropyltriethoxysilane >98% was purchased from Fluka.

- 3-mercaptopropyltrimethoxysilane >98% was purchased from Fluka.

- Toluene 98% was purchased from Lab Scan.

- Membrane filter, Qualitative circles 90 mm. diameter was purchased from Whatman.

3.1.4 High performance liquid chromatography (HPLC) condition

- **Chemical reagents**

    - Acetonitrile was purchased fromLAB SCAN.

    - Methanol was purchased fromLAB SCAN.

- **Materials**

    - ColumnC18 (ZORBAX Eclipse XDB-C18 2.1 x 100 mm (3.5μm), Agilent, USA)

    - SPE (Solid Phase Extraction)

    - C18 Cartridge(500 mg/3 ml, Cleanert ODS-SPE)

    - Membrane filter GF/C (25 mm, 0.12 μm, Whatman)

    - Membrane filter Nylon (0.45 μm, National Scientific)

    - Syringe filter)Nylon, Filtrex)

High performance liquid chromatography (HPLC) equipped with a photodiode array detector (230 nm). The C18 column 2.1 x 100 mm (3.5 μm) was used in this study. The elution gradient was conducted by using water (A) and acetonitrile (B), which initial condition of mobile phase B 100% v.v^{-1} reach to 70% in 5 min, flow rate was 1 mL/min.

3.1.5 Modified High Gradient Magnetic Separation Filtration

- **Chemical reagents**

    - Ethanol (Absolute) AR. grade was purchased from RCI Labscan.

    - Hexamethyldisilazane 98% was purchased from Acros Organics.

    - Tetraethoxysilan reagent grade 98% was purchased from Aldrich.

3.2 Methods

    3.2.1 Synthesis of adsorbents

        ● Synthesis of superparamagnetic hexagonal mesoporous silicates (HMS-SP)

Superparamagnetic iron oxide particles (SP) was synthesized as the core-shell of the adsorbent via co-precipitation from aqueous alkaline solutions as described by (Hongsawat, 2013) with some modification. In a typical synthesis, $FeCl_3.6H_2O$ (0.046 mol) and $FeSO_4.7H_2O$ (0.023 mol) were dissolved in 150 ml de-ionized water. Then, 20 ml ammonium hydroxides (25%) was added quickly into the mixture solution at 80°C. The SP (Fe_3O_4) was collected through magnetic separation and washed with de-ionized water five times. A solution of 10% ammonium salt of oleic acid (pH 10) was prepared by mixing 30 ml de-ionized water, 3 ml oleic acid, and 30-40 drops NH_4OH (30%w/w). This solution is added to the slurry drop wise under constant stirring at 60°C until the slurry changes into a stable suspension.
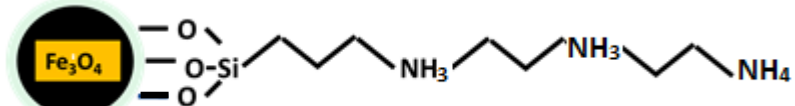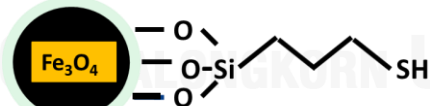
Pristine superparamagnetic hexagonal mesoporous silica (HMS-SP) was prepared following the previous method (H. Tian et al., 2009). A 0.50 g of SP was dispersed in 250 ml of 0.1 M HCl aqueous solution by ultrasonication for 10 min and this obtained material were separated and washed with de-ionized water by magnetic separation. The as-treated SP was added into the mixture solution of a dodecylaminde (0.35 g), ethanol (3.94 g) and water (27.36 g). The mixture were stirred at room temperature for 0.5 hr. Then, a 2.0 g of tetraethoxysilane (TEOS) was added drop wise to the mixture under vigorous stirring at room temperature for 24 hr. After that the material was collected with an external magnetic and washed with de-ionized water and ethanol to remove nonmagnetic by-products. Subsequence, the

obtained powders were extracted by refluxing with ethanol (200 ml) at 80 $^{\circ}$C for 12 hr twice times to remove the surfactant templates.

- **Functionalized superparamagnetic hexagonal mesoporous silicates (HMS-SP): post-grafting method**

The grafting method was synthesized following process. 0.5 g of HMS-SP was dehydrated in oven at 105℃ 24hr. Then HMS-SP stirred with 30 ml of toluene and 1 g of each organosilane at room temperature for 24 hr. The products were filtrated and washed with toluene. Lastly, the products were dried in oven at 85℃ 2 hr. The applied organosilanes in this study is 3aminopropyltriethoxysiliane and 3mercaptopropyltriethoxysilane) that show in **Table 3.1**.

Table 3. 1 Surface functional groups structure of adsorbents

Adsorbents	Chemical structures	Functional groups
HMS-SP		Silanol (SiOH)
3N-HMS-SP		Amino (N$_3$H$_{10}$) Silanol (SiOH)
M-HMS-SP		Mercapto (SH) Silanol (SiOH)

3.2.2 Characterization of adsorbents

To determine the physicochemical characteristic properties of adsorbents, the adsorbents were analyzed following the procedure in **Table 3.2.**

Table 3. 2 Instruments and parameters of the physicochemical characteristics of adsorbents

Instruments	Parameters
• X-ray Diffractometer (XRD)	• Silica structure
• Fourier Transform Infrared Spectroscopy (FT-IR)	• Surface functional group
• Nitrogen adsorption-desorption isotherm using BET theory	• Surface area and pore size
• Zeta potential analyzer	• Surface charge
• Elemental analyzer	• Quantity of total Nitrogen (N) and Sulfur (S)
• Laser particle analyzer	• Particle size

3.2.2.1 Silica structure

Crystal structure and crystal size were measured by Low-angle Powder X-ray diffraction (XRD), (Bruker AXS, D8 Discover) with Cu Kα X-ray type at scanning rate 1,000 deg min^{-1} between $0.5^{\circ} - 6.0^{\circ}$ (2θ). Before analysis, the sample was heated at 105°C in oven for 24 hr, and kept in desiccators.

3.2.2.2 Surface functional group

Surface functional groups were measured by Fourier Transform Infrared spectrometer (FTIR) and the spectra in the transmittance mode during 400-4000 cm^{-1}. Preparation of sample by mixed the adsorbent with KBr and then the sample was heated at 105°C in oven for 24 hr, and kept in desiccators.

3.2.2.3 Surface area and pore size

Surface area and pore size was calculated from nitrogen adsorption isotherms measured at 77 K by using an Autosorb-1 Quantachrome automatic volumetric sorption analyzer. Before analysis, the adsorbents were heated at 105°C in oven for 24 hr, and kept in desiccators. Whereas the specific surface area, pore diameter and pore volume was calculated by using the Brunauer-Emmett-Teller (BET) theory. Pore size distribution was calculated by using the Barrett-Joyner-Halenda (BJH) equation.

3.2.2.4 Surface charge

Surface charge was measured by acid-base titration. Preparation of sodium hydroxide solution (NaOH), 0.025 M of hydrochloric solution (HCl), and 0.1 M of sodium chloride solution (NaCl) and then preparation of mixed solution from adsorbent and mixed solution in ratio 1 g/L (adsorbent 0.02 g/ mixed solution 20 mL). Each mixed solution have difference pH value (range 3 to 10) and adjusted by NaOH solution or HCl solution in 25 mL of volumetric flask and controlled in 0.01 M of ionic strength. The sample was diluted by de-ionized water until 25 mL after that shaken 200 rpm, 12 hr, and 25°C. Surface charge in unit (C/m^2) was calculated from pH value at equilibrium state in equation (4.1).

$$\text{Surface charge (C m}^{-2}) = \frac{\left\{[HCl]-[NaOH]-[H^+]+[OH^-]\right\}}{M \times S_{BET}} \times 96{,}500 \quad (4.1)$$

Where [HCl]   =   Concentration of HCl to add (mol/L)

[NaOH]   =   Concentration of NaOH to add (mol/L)

[H$^+$]   =   Concentration of photon ion (mol/L)

Calculation from pH = -log [H$^+$]

[OH$^-$]   =   Concentration of hydroxide ion (mol/L)

                 Calculation from pOH = -log [OH$^-$] and

                 pOH= 14-pH

96500   =   Faraday's constant (C/mol)

M   =   Weight of adsorbent (g/L)

S_{BET} =   Surface of adsorbent (m^2/g)

3.2.2.5 Nitrogen and sulfur content

Nitrogen and sulfur content from amino and mercapto functional groups respectively were measured by CHNSO and LECO SC132 sulfur analyzer at Analytical and Testing Service Center, Petroleum and Petrochemical College, Chulalongkorn University. For analysis, the sample 0.3 g. was heated at 1,350 °C under static condition and calculated the content of total nitrogen and sulfur in percentage of weight by weight (%wt/wt) by compare with standard of nitrogen and sulfur.

3.2.2.6 Particle size

Particle size was measured by laser particle size distribution analyzer (MALVERN, Mastersizer S).

3.2.3 Adsorption experiment

3.2.3.1 Removal of Clofibric acid at high concentration

- **Adsorption kinetic study**

Adsorption kinetics were set by varying the contact time and initial CFA concentration at 10 mg/L and 1 g/L of adsorbent in 0.002 M phosphate buffer

pH 7.0. The samples were shaken at 200 rpm at room temperature, and then the solutions were filtrated through a nylon syringe filter (pore size 0.45 nm). Then, the remaining CFA concentration was analyzed by high performance liquid chromatography (HPLC) equipped with a photodiode array detector (230 nm).

- **Adsorption isotherm study**

      Adsorption isotherms were conducted with an initial CFA concentration range between 6-15 mg/L and 1 g/L of adsorbent. The ionic strength of the solutions were fixed using 0.002 M phosphate buffer at either pH 5, 7 or 9. The samples were shaken at 200 rpm at room temperature until the equilibrium are reached, and then the solutions were filtrated through a nylon syringe filter (pore size 0.45 nm). The remaining CFA concentration in equilibrium solutions were analyzed by high performance liquid chromatography (HPLC) equipped with a photodiode array detector (230 nm).

3.2.3.2 Removal of Clofibric acid at low concentration

- **Adsorption isotherm study**

Adsorption isotherms were conducted with an initial CFA concentration range between 50-200 µg/L and 1 g/Lof adsorbent. The ionic strength of the solutions were fixed using 0.002 M phosphate buffer at only one pH from removal of Clofibric acid at the same condition in environment. The samples were shaken at 200 rpm at room temperature until the equilibrium are reached, and then the solutions were filtrated through a nylon syringe filter (pore size 0.45 nm). The remaining CFA concentration in equilibrium solutions were analyzed by a solid phase

extraction (SPE) and high performance liquid chromatography (HPLC) equipped with a photodiode array detector (230 nm).

- **Solid phase extraction (SPE)**

The C18 cartridges (500mg/3mL) were used in solid phase extraction (SPE). The cartridge was equilibrated with 5 mL of methanol and 10 mL of de-ionized water. Then the sample was collected, washed with 10 mL of de-ionized water and eluted with 10 mL of methanol. Finally, the sample was evaporated and adjusted to 0.5 mL of methanol that shows as **Figure 3.1**.
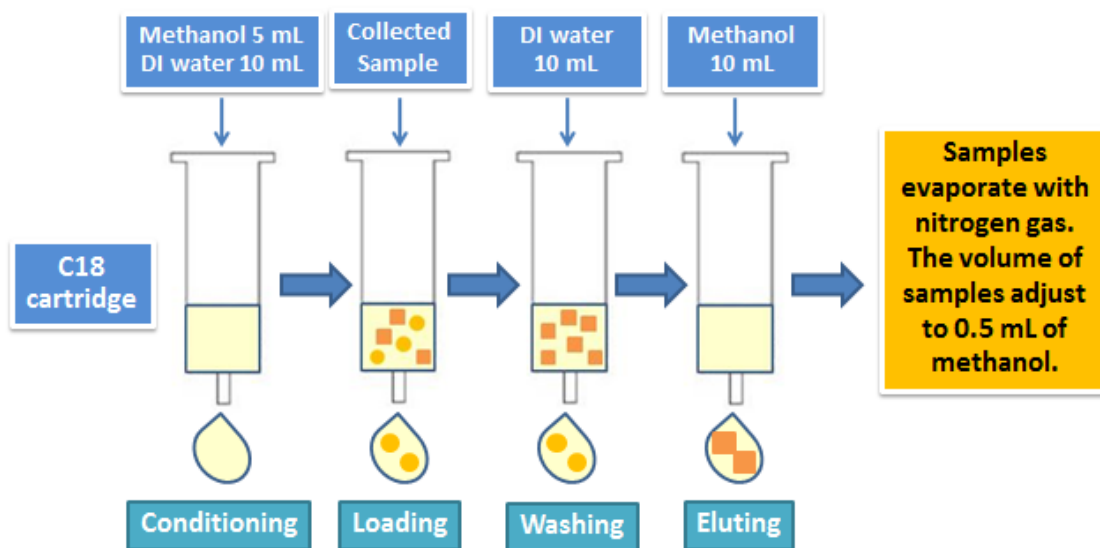
Figure 3. 1 Condition of solid phase extraction (SPE)

- **High Performance Liquid Chromatography (HPLC)**

The sample was measured by high performance liquid chromatography (HPLC) equipped with a photodiode array detector (230 nm). The C18 column 2.1 x 100 mm (3.5 μm) was used in this study. The elution gradient was conducted by using water (A) and acetonitrile (B), which initial condition of mobile phase B 100% $v.v^{-1}$ reach to 70% in 5 min, flow rate was 1 mL/min. The detection limit of concentrated sample was 50 µg/L with SPE. The recovery percentage was

approximately 95% without NOM, and the recovery standard deviation percentage (%RSD) was 2.62%. Chromatogram of CFA was shown in **Figure 3.2**.
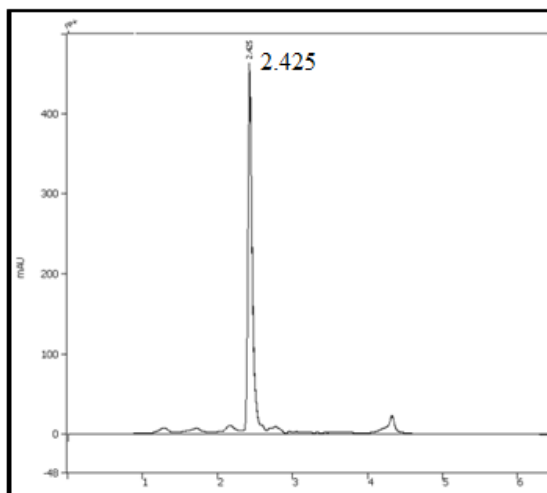
Figure 3. 2 Chromatogram of Clofibric acid at 8 mg/L, pH7

3.2.3.3 Removal of Clofibric acid from real wastewater

- **Fractionation of natural organic matter (NOM)**

The background NOMs in real wastewater sample was fractionated from one swine farm in northern part of Thailand. Before separation of natural organic matter (NOM) by fractionation, collected sample was filtered through a glass filter (GC/F, pore size 0.75μm) and adjusted with H_2SO_4 to pH 2. Then, collected sample was fed through resin (DAX-8), flow rate 20 mL/min. Water sample that was released from column in the first time, is hydrophilic NOM component. Eluting of hydrophobic NOM component by 0.1 N of NaOH 25 mL and 0.01 N of NaOH 125 mL, flow rate 200 mL/min. Clofibric acid (CFA) was prepared by de-ionized water at concentration 100 mg/L. After that it was diluted by fractionated wastewater as stock solution. Finally, there are two components to separation such as hydrophobic and hydrophilic NOM and using in this section.

Table 3. 3 The properties of natural organic matter (NOM)

Parameter	Hydrophobic fraction	Hydrophilic fraction	Non-fraction
pH	7.35	6.17	7.00
Conductivity (S/cm)	0.009	0.009	0.018
TOC (mg/L)	0.7189	0.7826	-

- **Adsorption isotherm study in the presence of NOMs**

Adsorption isotherm was conducted with an initial CFA concentration range between 6-15 mg/L and 1 g/L of adsorbent by using fractionate real wastewater. The sample was shaken at 200 rpm at room temperature, and then the solution was filtrated through a nylon syringe filter (pore size 0.45nm). The remaining CFA concentration in equilibrium solution was analyzed by high performance liquid chromatography (HPLC) equipped with a photodiode array detector (230 nm). The elution gradient was conducted by using water (A) and acetonitrile (B), which initial condition of mobile phase B 100% $v.v^{-1}$ reach to 0% in 10 min, flow rate was 1 mL/min. **Figure 3.3** shows the chromatogram of CFA and NOM in hydrophobic (HPO) and hydrophilic (HPI) fractions compare with the peak of CFA.
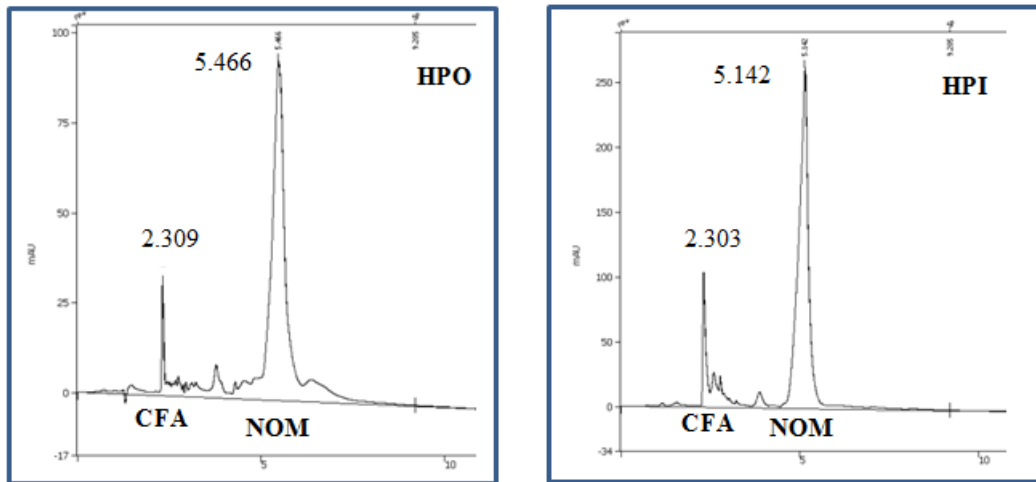
Figure 3. 3 Chromatogram of CFA in hydrophobic (HPO) and
hydrophilic (HPI) fractions

3.2.2 High Gradient Magnetic Separation Filtration

The magnetic filtration column consist of wire stainless filter, acrylic pipe diameter 1.9 cm, and high 7 cm, stainless fiber, and hydraulic pump that shows as **Figure 3.4** and **Figure 3.5** (Ruangtrakul, 2010).
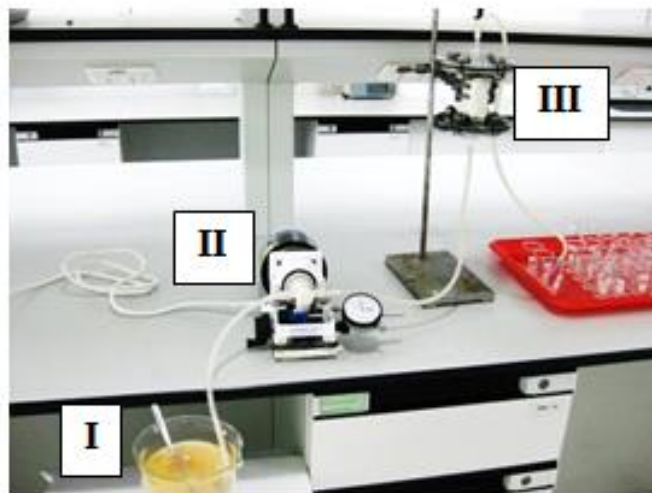
Figure 3. 4 The filtration system: I-Stirrer, II-Pump, III-Magnetic filtration
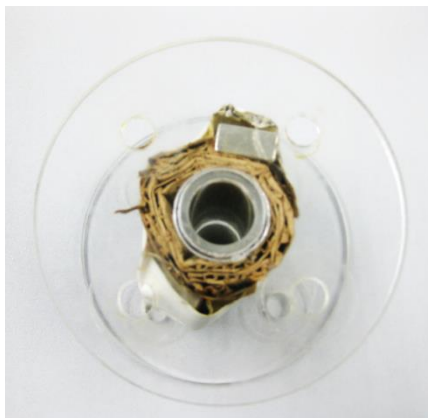
Figure 3. 5 Column of high gradient magnetic separation filter

Hydrophobic stainless fiber surface modified filter

Hydrophobic surface modified filter was conducted by coating wire stainless with silica sol solution as described by (Bhagat, 2006; Lortragool, 2009) with some modification due to increasing the retention efficiency to trap the adsorbent particle which hydrophilic adsorbent in hydro phase (water). Silica sol solution was prepared by tetraethoxysilane, hexamethyldisilazane, ethanol, and de-ionized water in ratio of molar; 1:1:36.4:6.6. The mixture was stirred 5 min. After 45 min, the wire stainless was coated with silica sol solution and dried at room temperature. Then, wire stainless was fixed in magnetic filtration column. The modified wire stainless was shown in **Figure 3.6**.
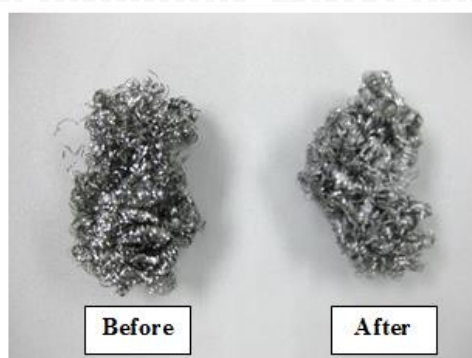
Figure 3. 6 Comparison between before and after modified wire stainless

Measurement method of suspended solid

First, collecting 25 mL of each sample from filtration column until the particle removal efficiency of HGMS filter is finished as in **Figure 3.7**. Then, collected samples were filtered by GC/F membrane filter. And filter paper was dried in oven at 105 ℃. Finally, The different weight of filter paper before and after filtration was used to calculate the removal efficiency of HGMS filter, as shown in **Figure 3.8**.
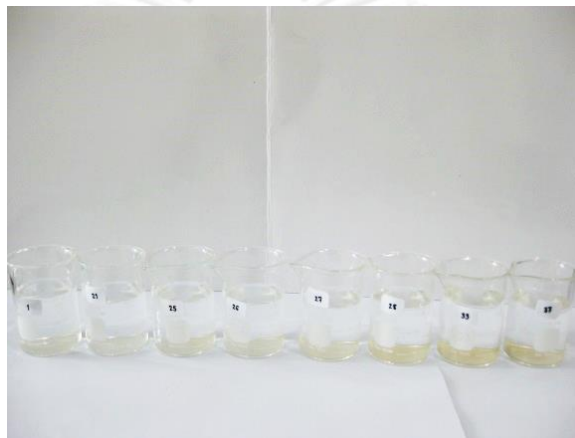
Figure 3. 7 Sample collecting

Figure 3. 8 After dried filter paper in oven

3.2.4.1 Effect of modified hydrophobic surface filter

To study effect of modified hydrophobic surface filter on separation process, the following step was conducted.

1. Mix synthesized adsorbent with de-ionized water in ratio 0.6 g of adsorbent per 1 Liter of de-ionized water.

2. Pump the mixed solution into the non-modified stainless fiber column under varying flow rate 5m/hr.

3. Collect the sample and measure the concentration of adsorbent by measuring suspended solids concentrate and the experiment will be conducted as same as previous study again with modified hydrophobic surface filter. This condition was summarized in **Table 3.3**.

Table 3. 4 The conditions of High Gradient Magnetic Filtration for studying the effect modified hydrophobic surface filter

Parameters	Values
Varied parameter	
• Surface filter	Modified hydrophobic surface filter/ non-modified hydrophobic surface filter
Controlled parameters	
• Adsorbent concentration	
• Flow rate	0.6 g/L
• Depth filter	5 m/hr
• Surface area filter	7 cm
	222.22 cm^2 (1.5 g of wire stainless)

3.2.4.2 Effect of flow rates

To study effect of flow rate on separation process, the following step will be conducted.

1. Mix synthesized adsorbent with de-ionized water in ratio 0.6 g of adsorbent per 1 Liter of de-ionized water.

2. Pump the mixed solution into the column under varying flow rate 3, 5, and 7 m/hr respectively.

3. Collect the sample and measure the concentration of adsorbent by measuring suspended solids concentrate. This condition was summarized in **Table 3.4**.

Table 3. 5 The conditions of High Gradient Magnetic Separation Filtration for studying the effect of flow rates

Parameters	Values
Varied parameter	
• Flow rate	3, 5, and 7 m/hr
Controlled parameters	
• Adsorbent concentration	0.6 g/L
• Depth filter	7 cm
• Surface area filter	222.22 cm^2 (1.5 g of wire stainless)
• Stainless fiber	Non-modified stainless

3.2.4.3 Effect of concentration of adsorbent

To study effect of concentration of adsorbent on separation process, the following step will be conducted.

1. Mix synthesized adsorbent in de-ionized water by varying ratio of adsorbent from 0.3, 0.6, and 1 g per 1 Liter of de-ionized water, respectively.
2. Pump the mixed solution into the column at flow rate 5 m/hr.
3. Collect the sample and measure the concentration of adsorbent by measuring suspended solids concentrate. This condition was summarized in **Table 3.5**.

Table 3. 6 The conditions of High Gradient Magnetic Separation Filtration for studying the effect of concentration of adsorbent

Parameters	Values
Varied parameter	
• Adsorbent concentration	0.3, 0.6, and 1 g/L
Controlled parameters	
• Flow rate	5 m/hr
• Depth filter	7 cm
• Surface area filter	222.22 cm^2 (1.5 g of wire stainless)
• Stainless fiber	Non-modified stainless fiber

3.2.5 Iron release

The iron (Fe) concentration in the solutions at equilibrium state from adsorption study of each adsorbent was measured by Atomic Absorption Spectrometer (AAS). Each experiment was conducted under the same adsorption condition in 0.002 M. of phosphate buffer pH 7 and 25 $^\circ$C.

CHAPTER IV
RESULTS AND DISCUSSION

4.1 Characterization of physico-chemical properties of adsorbents

All adsorbents were characterized physio-chemical properties such as X-ray diffraction (XRD), Fourier Transform Infrared Spectrometer (FTIR), Nitrogen adsorption-desorption isotherms, pH at point of zero charge (pH_{zpc}), CHONS Elemental analyzer, and particle size. These parameters were used to analyzed the adsorption mechanism of CFA on HMS-SPs.

4.1.1 X-ray diffraction (XRD)

X-ray diffraction was used to determine crystalline structure of mesoporous structure at 2Θ angel of 0.5°-10.0° as shown in Figure 4.1. As a result, the XRD diffraction pattern of HMS-SP showed only one reflection corresponding at 2Θ = 1.43° that referred to the hexagonal mesoporous silica structure of HMS-SP. However, the obtained peak has low intensity and board shape, which mean that the hexagonal mesoporous structure might be non-uniformity structure. The collapsed structure of HMS-SP might be cause by adding of superparamagnetic particle into mixture before adding silica precursor to form porous structure during synthesis process.
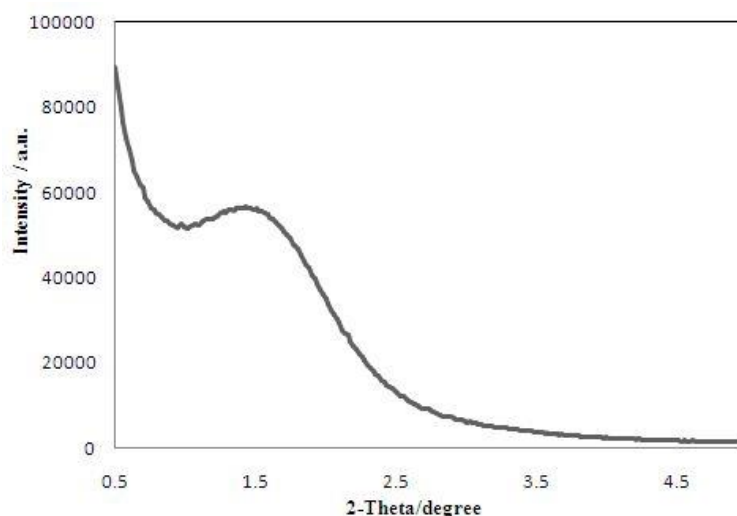
Figure 4. 1 XRD pattern of HMS-SP

4.1.2 Fourier Transform Infrared Spectrometer (FTIR)

Surface functional groups of synthesized adsorbents (HMS-SP and functionalized HMS-SPs) on the adsorbents surface can be confirmed by using FTIR spectroscopy that showed in **Figure 4.2**.

All of adsorbents spectra performed the O-H stretching of free silanol group at 3742 cm^{-1} and the peak at 3435 cm^{-1} indicated the hydrogen boned hydroxyl group (O-H stretching). C-H stretching on the surfaces can be confirmed by the peak at 2950 cm^{-1}. The asymmetric Si-O-Si at 1000-1200 cm^{-1}, the symmetric Si-O-Si at 804-814 cm^{-1}, and the O-Si-O stretching at 460 cm^{-1} indicated that all adsorbents have silanol and ring structure of Si-O$_4$ on surface. In the case of 3N-HMS-SP amino group can be indicated by the peak at 1580-1680 cm^{-1} of N-H bending. For M-HMS-SP, mercapto group should have the peak of S-H stretching at 2490-2580 cm^{-1}. Unfortunately, the board peak of hydrogen boned hydroxyl group (O-H stretching) at 3435 cm^{-1} could interfere the peak of S-H stretching. Therefore, the presence of mercapto group has to be confirmed by total sulfur content that can be measured by CHONS elemental analyzer.
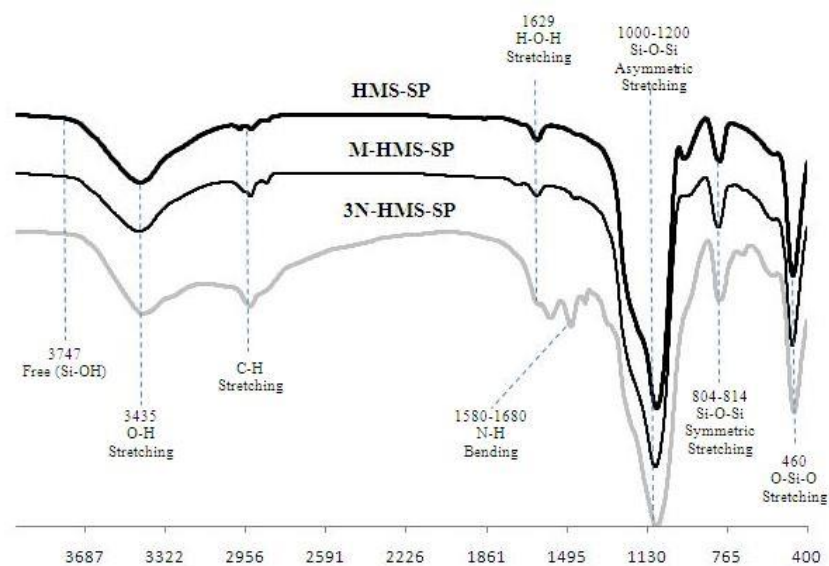
Figure 4. 2 FTIR spectra of HMS-SP and

functionalized HMS-SPs

4.1.3 Nitrogen adsorption-desorption isotherms

Nitrogen adsorption-desorption isotherms were used to determine pore size, pore volume, and surface area of all adsorbents. The surface area of all adsorbents was calculated from Brunauer-Emmett-Teller (BET) isotherm and the pore size distribution and the pore volume were calculated from Barrett-Joyner-Halenda (BJH) method. The nitrogen adsorption-desorption isotherms and pore size distribution of HMS-SP and functionalized HMS-SP are shown in **Figure 4.3**, **Figure 4.4**, and **Table 4.1**. The isotherms of HMS-SP and functionalized HMS-SPs were type IV isotherm (Sing, 1982) and showed that the BET surface area and the pore volume of the adsorbents followed the order: M-HMS-SP>HMS-SP>3N-HMS-SP. Surface area and pore volume of 3N-HMS-SP was decreased due to the grafting of functional group inside the pore. However, surface area of M-HMS-SP was not changed significantly, but pore diameter together with pore volume of M-HMS-SP was decreased by grafting mercapto functional group. It can be indicated that mercapto functional group was grafted at the surface both internal and external surface. The calculated pore sizes of HMS-SP, M-HMS-SP, and 3N-HMS-SP were 93.54, 79.35, and 128.2,

respectively. The highest pore size is 3N-HMS-SP that might be caused by the destruction of the silica structure during the grafting with functional group. Comparing between the pore size of synthesized adsorbents and molecular size of CFA, it was found that CFA can access and interact with surface functional groups both inside and outside of adsorbent porous structures.
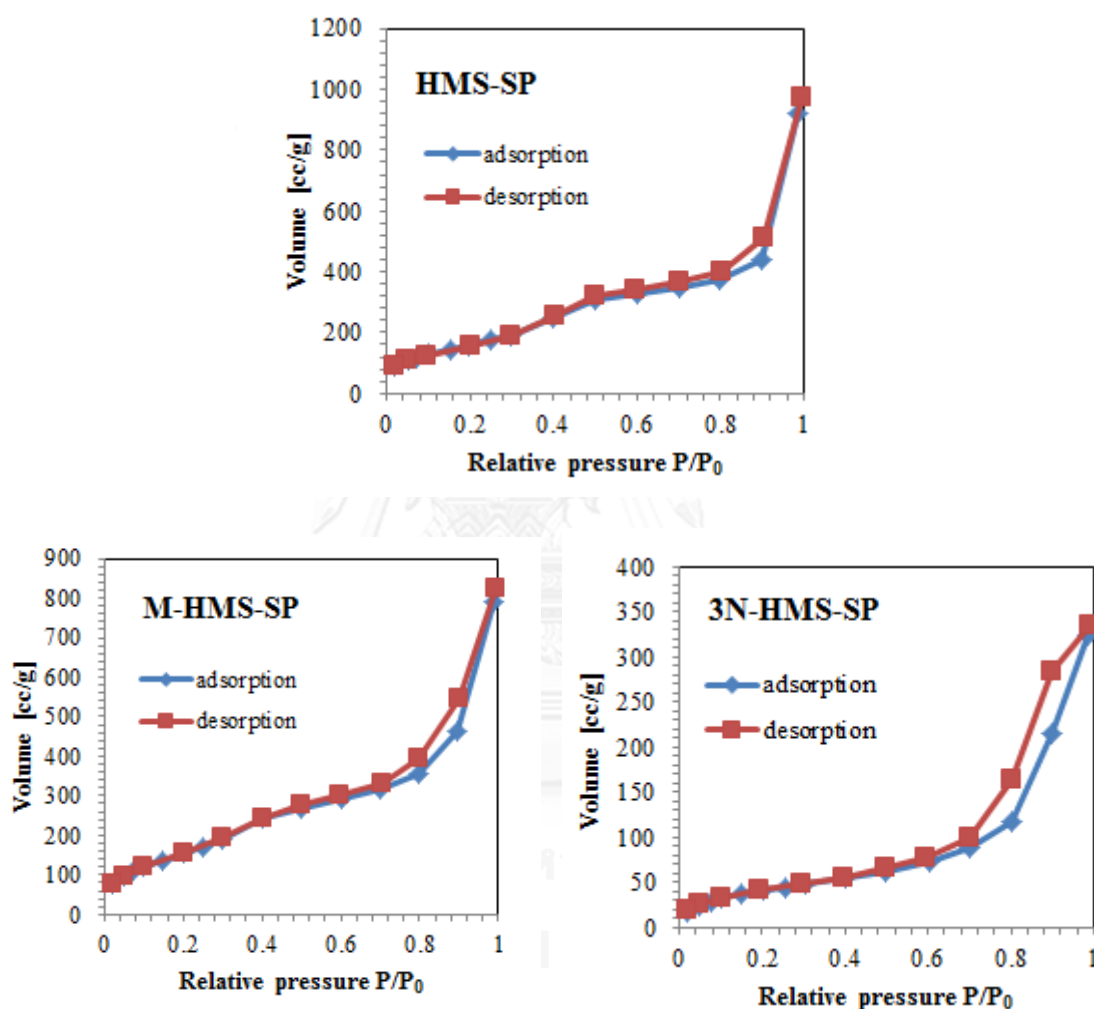
Figure 4. 3 Nitrogen adsorption-desorption isotherms of HMS-SP and functionalized HMS-SPs
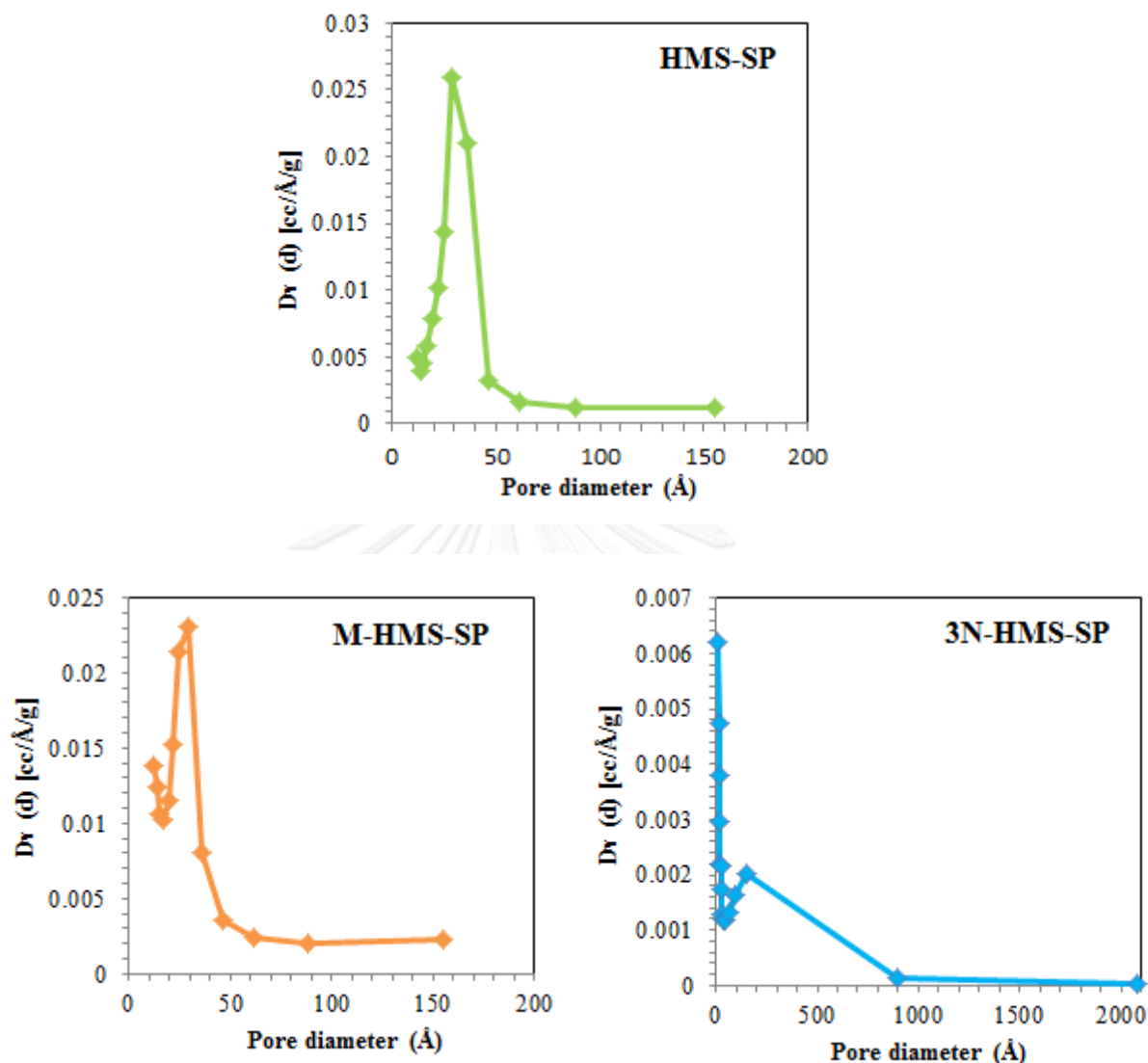
Figure 4. 4 Pore size distribution of HMS-SP and functionalized HMS-SPs

Table 4. 1 Parameters from the N_2 adsorption-desorption isotherms

Adsorbents	Surface functional groups	Pore diameter (nm)	Pore volume (cc/g)	BET surface area (m^2/g)
HMS-SP	Silanol	9.4	1.429	611
M-HMS-SP	Silanol and mercapto	7.9	1.226	618
3N-HMS-SP	Silanol and amino	12.8	0.5006	156
PAC	abonyl, phenyl and oxygen containing groups	1.90	276	980

4.1.4 pH at point of zero charge (pH_{zpc})

pH at point of zero charge of synthesized adsorbents were determined by acid-base titration method. The pH_{zpc} of each adsorbent are shown in **Figure 4.5**, **Table 4.2**. According to the result, the pH_{zpc} of all adsorbents were depended on the surface functional group of each adsorbent; HMS-SP, M-HMS-SP, and 3N-HMS-SP were 5.9, 6.1, and 9.5, respectively.
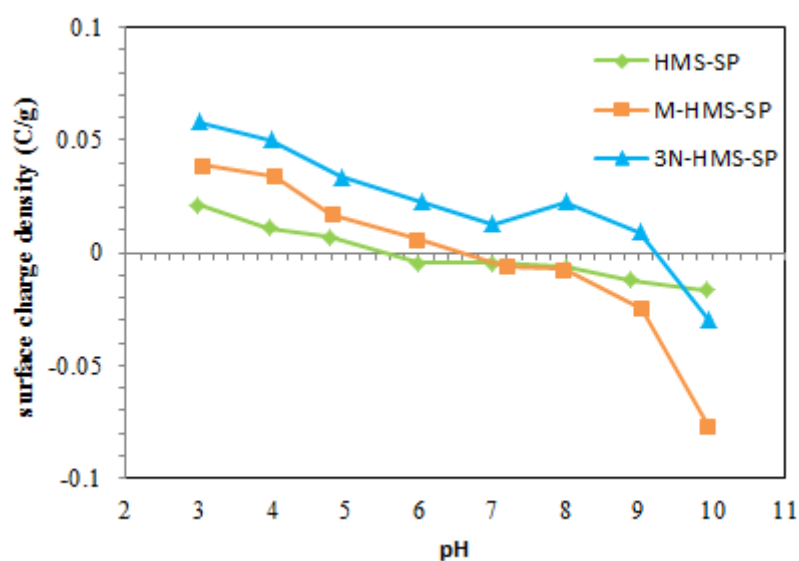
Figure 4. 5 Surface charge density of HMS-SP and functionalized HMS-SPs

Table 4. 2 The pH_{zpc} of HMS-SP and functionalized HMS-SPs

Adsorbents	pH_{zpc}
HMS-SP	5.7
M-HMS-SP	6.6
3N-HMS-SP	9.2

4.1.5 CHONS Elemental analyzer

The CHONS elemental analyzer was used to measure the total nitrogen and sulfur content on surface in adsorbents. The total nitrogen content on 3N-HMS-SP surface was 75.19 $\mu mol_N.m^2$ and total sulfur content on M-HMS-SP surface was

1.9460 $\mu mol_S.m^2$ that shown in **Figure 4.6** and it can confirm the presence of grafted functional group on surface of 3N-HMS-SP and M-HMS-SP, respectively.
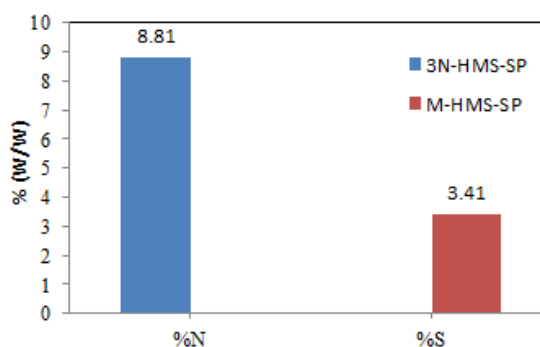
Figure 4. 6 Content of total nitrogen and sulfur of functionalized HMS-SPs

4.1.6 Particle analyzer

The particle size of synthesized adsorbents was determined by laser particle analyzer. The particle size of each adsorbent is shown in **Table 4.3**. According to the results, the particle size of all adsorbents were depended on the modification of surface adsorbent due to the functionalization was destroys adsorbent structures; HMS-SP, M-HMS-SP, and 3N-HMS-SP particle diameters were 133.52, 28.80, and 44.70 µm, respectively.

Table 4. 3 The particle size of HMS-SP and functionalized HMS-SPs

Adsorbents	Particle diameter (µm)
HMS-SP	133.52
M-HMS-SP	28.80
3N-HMS-SP	44.70

4.2 Adsorption experiments

4.2.1 Adsorption at high concentration

4.2.1.1 Adsorption kinetic

Adsorption kinetic of CFA was conducted at initial concentration of 10 mg.L^{-1} and pH 7 controlled by phosphate buffer 2mM, 25°C. The ratio of adsorbent to adsorbate was fixed at 1 g.L^{-1}. The samples were collected during 0-24 hr. According

to **Figure 4.7**, CFA adsorption capacities (mg/g unit) were rapidly increased in 1 hr and approached to equilibrium within 6 hr for HMS-SP, 3N-HMS-SP, and M-HMS-SP, while 2 hr for PAC.
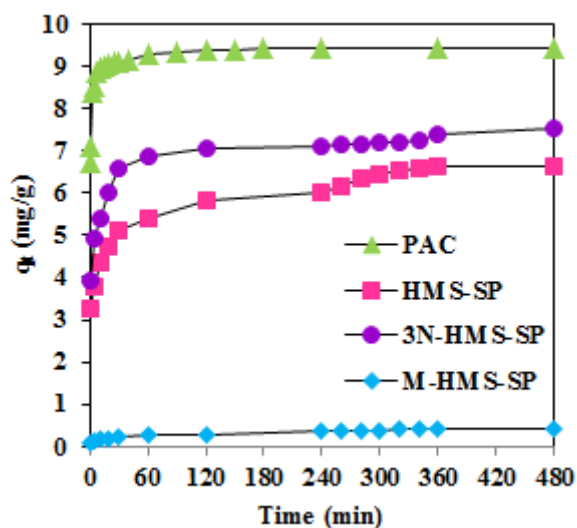
Figure 4. 7 Adsorption kinetics of CFA by HMS-SP, functionalized HMS-SPs, and PAC at initial concentration 10 mg/L, pH 7, and IS 2 mM

The adsorption rate of PAC was clearly faster than synthesized adsorbents, which might be caused by the surface functional group complexity and higher pore accessibility due to very board pore size distribution of PAC. Although, the mean pore size of PAC was smallest comparing with the synthesized adsorbents, the ratio of large pore (mega pore) of PAC was extremely high comparing with HMS-SPs. M-HMS-SP had lowest adsorption capacity comparing with HMS-SP and 3N-HMS-SP and also supposed to have lowest adsorption rate.

Two types of adsorption kinetic models were used for modeling the adsorption kinetic of CFA adsorptions which are pseudo-first-order and pseudo-second-order kinetic models. The pseudo-first order kinetic model can be determined from equation (4.1);

$$\frac{1}{q} = \frac{k1}{q_e t} + \frac{1}{q_e} \qquad (4.1)$$

Where q_t is the amount of adsorbed (mg.g^{-1}) at time t (min), q_e is the amount of adsorbed (mg/g) at equilibrium and k_1 is the pseudo-first order rate (mg.g^{-1}). The values of k_1 and q_e are calculated from slope and intercept of the plots between 1/q and 1/t.

The pseudo-second order kinetic model can be determined from equation (4.2);

$$\frac{t}{q_t} = \frac{1}{k_2 q_e^2} + \frac{t}{q_e} \qquad (4.2)$$

Where k_2 is the pseudo-second order rate constant (g.mg^{-1}. h^{-1}) is calculated from the plots between t/q_t and t. According to the pseudo-second-order model, the initial adsorption rate (h) (mg. g^{-1}. h^{-1}) can be determined according to Equation (4.3);

$$h = K_2 qe^2 \qquad (4.3)$$

Table 4. 4 Kinetic parameters of CFA adsorption on HMS-SP, functionalized HMS-SPs, and PAC

Adsorbents	$q_{e,exp}$ (mg/g)	Pseudo-first-order			Pseudo-second-order			
		$q_{e,cal}$ (mg/g)	K_1 (g/mg. h)	R^2	$q_{e,cal}$ (mg/g)	K_2 (g/mg. h)	h (mg/g. h)	R^2
HMS-SP	6.72	3.12	0.532	0.959	6.75	0.732	33.35	0.998
3N-HMS-SP	7.45	1.77	0.448	0.829	7.46	1.497	83.31	0.999
M-HMS-SP	0.43	0.32	0.435	0.952	0.43	4.481	0.83	0.985
PAC	9.44	0.88	1.337	0.913	9.52	11.034	1000.02	1.000

Obtained kinetic data were fitted by pseudo-first-order and pseudo-second-order models that shown in **Table 4.4**. All kinetic experiments are matched with pseudo-second-order model and rate of adsorption followed in order of affinity adsorption; PAC>3N-HMS-SP>HMS-SP>M-HMS-SP. The adsorption phenomena of CFA on all adsorbents were investigated by intraparticle diffusion model of Weber and Morris theory that can be expressed as equation (4.4);

$$q_t = k_{IPi}.t^{0.5} + C_i \qquad (4.4)$$

Where q_t, k_{IPi}, and C_i are the amount adsorbed at time t (mg/g), the intraparticle rate constant of stage i (mg/g.h$^{-0.5}$), and the intercept of stage i, respectively.
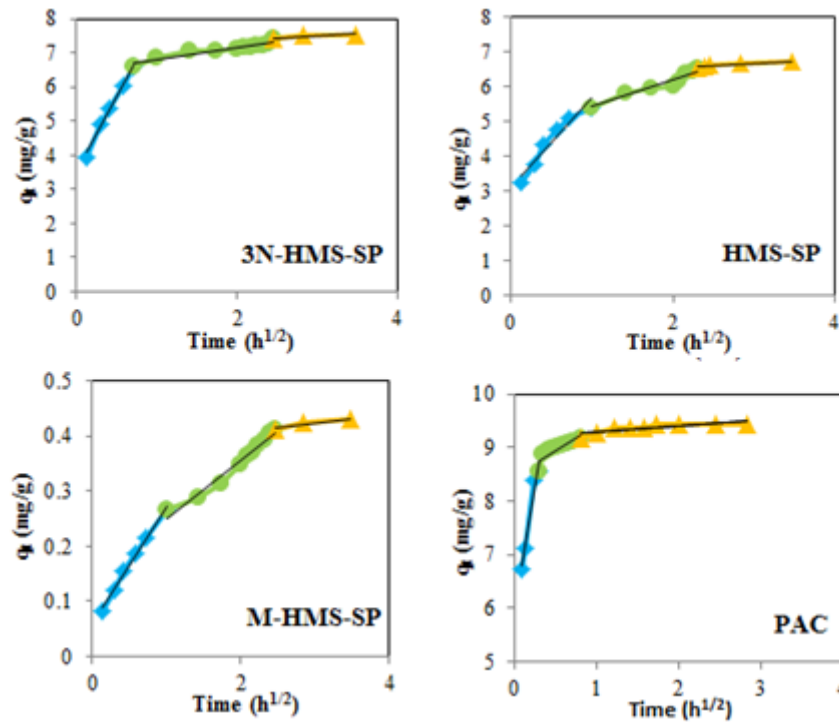
Figure 4. 8 Weber and Morris equation plots of CFA adsorbed onto HMS-SP, functionalized HMS-SPs, and PAC

Figure 4.8 indicated the plot of Weber and Morris equation (equation 4.4) of all adsorbents. From obtained results **(Figure 4.8)**, this suggests that CFA adsorption phenomena are consist of three steps for all adsorbents. The first step represents film diffusion process that CFA from solution diffuse into external surface of the adsorption. The second step represents intraparticle diffusion process that CFA diffuse into pore of adsorbent. The third step represents the equilibrium of adsorption. According to the straight lines did not pass through the origin that means all applied adsorbents are favorable to CFA.

4.2.1.2 Adsorption isotherm

4.2.1.2.1 Adsorption isotherm models

The adsorption isotherms were used to investigate the adsorption mechanism and predominant factors controlling the adsorption. The adsorption isotherm of CFA was conducted at initial concentration during 6-15 mg/L controlled by phosphate buffer 2 mM at pH 5, 7, and 9 (25°C). The adsorption isotherm models consist of Linear, Langmuir, and Freundlich isotherm were used to determine the CFA adsorption on adsorbent. The linear isotherm is given by equation (4.5);

$$q_e = K_p C_p \qquad\qquad (4.5)$$

q_e is the amount of adsorbate adsorbed at equilibrium (mg.L^{-1}) and K_p is the linear constant (L.mg^{-1}). C_e is the concentration of adsorbate at equilibrium (mg.L^{-1})

The Langmuir isotherm of linear form is calculated according to the following equation (4.6);

$$\frac{1}{q_e} = \frac{1}{q_m} + \frac{1}{k_{L}q_m C_e} \qquad\qquad (4.6)$$

Where k_L is the Langmuir constant (L.mg^{-1}) and q_m is the maximum adsorption capacity (mg.g^{-1}).

The Freundlich isotherm of linear form is calculated according to the following equation (4.7);

$$\ln q_e = \ln k_F + \frac{1}{n} \ln C_e \qquad\qquad (4.7)$$

Where k_F is the Freundlich constant and n is the adsorption intensity (dimensionless)

Table 4. 5 Isotherm parameters of CFA adsorption at high concentration pH 7, 25°C, IS 2 mM

Adsorbents	Freundlich				Langmuir			Linear	
	1/n	n	K_f	R^2	K_L (L/mg)	q_m (mg/g)	R^2	K_p (L/mg)	R^2
HMS-SP	1.060	0.943	1.301	0.966	0.003	454.546	0.959	1.592	0.963
M-HMS-SP	0.587	1.704	0.141	0.993	0.084	1.231	0.984	0.126	0.824
3N-HMS-SP	0.966	1.035	2.249	0.997	0.016	140.845	0.997	2.189	0.996
PAC	0.843	1.186	17.86	0.950	0.085	36.765	0.939	22.76	0.961

Adsorption isotherms of all adsorbents were fitted with Linear, Langmuir, and Freundlich isotherm model that shown in **Table 4.5**. According **Table 4.5**, the results of adsorption isotherms were mostly suitable with the Freundlich model. The Freundlich isotherm model is used to determine the characteristics adsorption for heterogeneous surface (Freundlich, 1906). The 1/n value is more than 1 that means a favorable adsorption process and the K_f value is an indicator of adsorption capacity. As a results of the CFA on adsorbents followed in order of affinity adsorption (base on K_f); PAC>3N-HMS-SP>HMS-SP>M-HMS-SP as shown in **Table 4.5**. The highest of K_f value in all synthesized adsorbents was 3N-HMS-SP due to adsorbent has hydrophilic interaction with CFA.

4.2.1.2.2 Effect of surface functional group

CFA adsorption isotherms of all adsorbents were used to determine the effect of surface functional group on CFA adsorption and functional groups consist of silanol, amino, and mercapto group. CFA adsorption isotherms of all adsorbents at pH 7 were shown in **Figure 4.9**, it is revealed that amino had the highest adsorption capacity following with silanol group and mercapto group, respectively. However, adsorption capacity of PAC was higher than all synthesized adsorbents. Van der waals interaction caused by hydrophobicity and surface functional group complexity are suggested to play the most important role for CFA adsorption on PAC surface. According to the results, 3N-HMS-SP and HMS-SP had adsorption capacities higher than M-HMS-SP which might relate to the hydrophilicity of adsorbents caused by hydrogen bonding, while M-HMS-SP is hydrophobic adsorbent. Furthermore, the

interaction between the CFA molecule and the synthesized adsorbents might relate to the electrostatic interaction. The pK_a of CFA is equal 3.81 (Loffler, 2005), hence CFA molecule should be ionized to be negative charge at pH 7. Hence, HMS-SP and M-HMS-SP, negative charge surface (at pH 7), should have the repulsive electrostatic interaction with CFA. This are supposed to decrease the CFA capacities of HMS-SP and M-HMS-SP to be less than 3N-HMS-SP and PAC, which had positive charge on surface in **Table 4.6**.
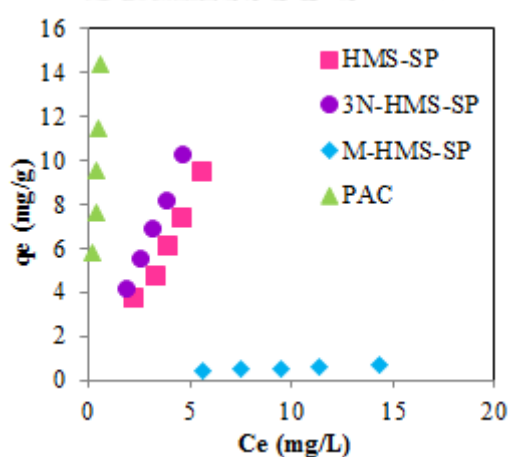
Figure 4. 9 Adsorption isotherms of HMS-SP, functionalized HMS-SPs,

and PAC at pH 7, 25°C, IS 2 mM

4.2.1.2.3 Effect of pH

Effect of pH on adsorption capacities of all adsorbents were determined by varying pH of solution during 5, 7, and 9 at IS 2 mM controlled by phosphate buffer **(Figure 4.10).** The experiments were studied the involvement between pH of solution and pH_{zpc} of adsorbent surface. If pH_{zpc} of adsorbent surface is lower than pH of solution, adsorbent surface functional groups are negatively charged that shows in **Table 4.6**. CFA adsorption isotherms at pH 5-9 were plotted and compared in **Figure 4.10**. Surprisingly, it was found that CFA adsorption capacities at pH 5, 7 and 9 of all synthesized HMS-SPs did not changed significantly, except for PAC. Hence, electrostatic interaction on carbonaceous surface of PAC was suggested to be stronger than silica structure of synthesized HMS-SPs. All synthesized adsorbents were positive charge at pH 5, while CFA was negative charge which might cause just

a little bit increase of CFA adsorption capacity on HMS-SPs by electrostatic interaction. Moreover, in case of 3N-HMS-SP, the surface was positively charged in the all pH (5 to 9), hence effect of electrostatic interaction on 3N-HMS-SP still cannot be concluded from this pH varying range. For PAC, the adsorption capacities were clearly enhanced by reducing pH due to expending attractive force of electrostatic interaction.

Table 4. 6 Relationship of charges between adsorbents and CFA

Adsorbents/ CFA	pH 5		pH 7		pH 9	
	Charge	Interaction	Charge	Interaction	Charge	Interaction
CFA	-		-		-	
HMS-SP	+	Attractive	-	Repulsive	-	Repulsive
M-HMS-SP	+	Attractive	-	Repulsive	-	Repulsive
3N-HMS-SP	+	Attractive	+	Attractive	+	Attractive
PAC	+	Attractive	+	Attractive	+	Attractive
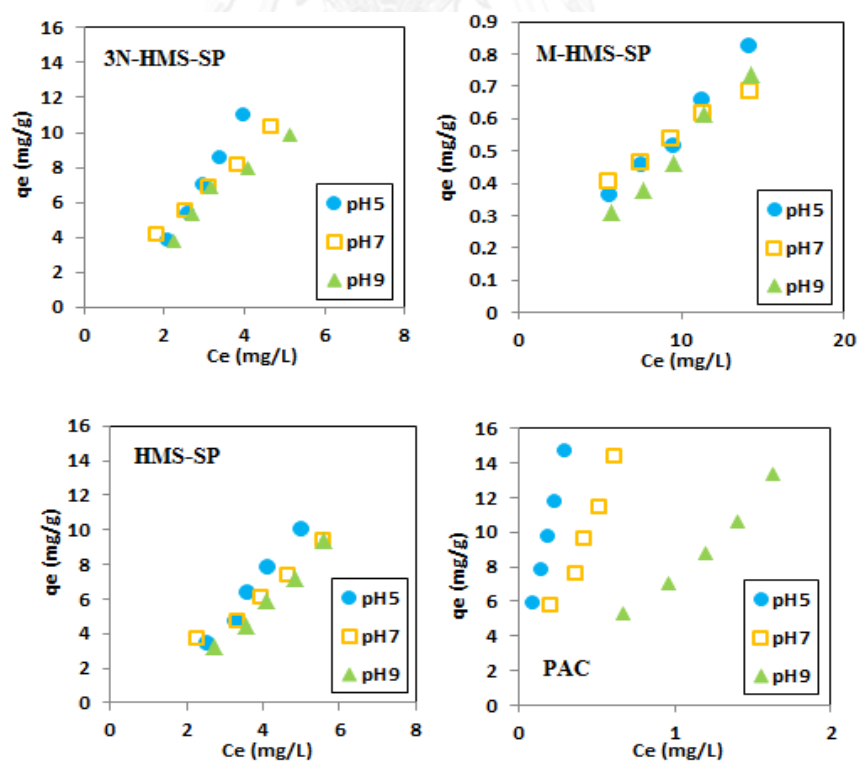
Figure 4. 10 CFA adsorption isotherms of HMS-SP, functionalized HMS-SPs,

and PAC at pH 5, 7, and 9

4.2.2 Adsorption at low concentration

The adsorption isotherm of CFA in low concentration was conducted at initial concentration during 50-200 µg/L controlled by phosphate buffer 2 mM at pH 7 (25°C) and the adsorbent was used in this section is 3N-HMS-SP due to the adsorption capacity of this adsorbent is highest. The results of adsorption isotherms were mostly suitable with the Freundlich and linear model that shown in **Table 4.7** and the percentage of CFA adsorption capacity at low concentration that it is nearly with CFA adsorption capacity at high concentration in the same condition that shown in **Figure 4.11**. Therefore, adsorption mechanism might be the same as the high concentration.

Table 4. 7 Isotherm parameters of CFA adsorption at low concentration pH 7, 25°C, Is 2 mM

Adsorbents	Freundlich				Langmuir			Linear	
	$1/n$	n	K_f	R^2	K_L (L/mg)	q_m (mg/g)	R^2	K_p (L/mg)	R^2
3N-HMS-SP	0.439	2.278	20.09	0.991	0.847	36.765	0.901	2.011	0.982
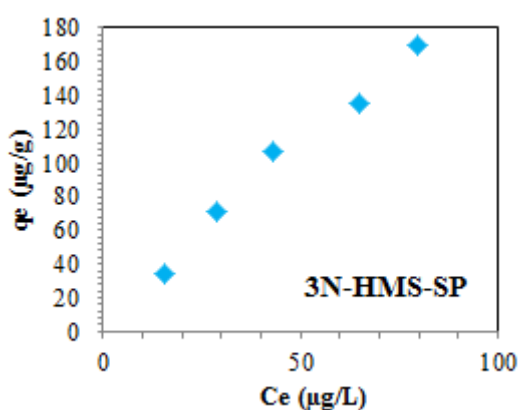
Figure 4. 11 CFA adsorption isotherm of 3N-HMS-SP at pH 7, 25°C, and IS 2 mM

4.2.3.1 Effect of hydrophobicity and hydrophilicity in real wastewater

The adsorption isotherms in real discharge wastewater from swine farm were used to investigate the adsorption mechanism and predominant factors controlling the adsorption in the real wastewater condition. The adsorption isotherm of CFA was conducted at initial concentration during 6-15 mg/L controlled by phosphate buffer 2 mM at pH 5, 7, and 9 (25°C) and 3N-HMS-SP was used in this section because of the highest adsorption capacity in high concentration section.

CFA adsorption isotherms in **Figure 4.12** were used to investigate the effect of hydrophobic and hydrophilic NOM in real wastewater on CFA adsorption capacities at pH 7. According to the results, synthetic CFA wastewater without NOM had the highest adsorption capacity following with the presence of hydrophobic and hydrophilic NOM, respectively. Sine, 3N-HMS-SP is hydrophilic adsorbent which might interact with the hydrophilic NOM via the hydrogen bonding easier than hydrophobic NOM.

On the other hand, CFA are supposed to have higher potential to interact with hydrophilic fraction than hydrophobic fraction of NOM. Hence, the multilayer adsorption between CFA and hydrophilic NOM on 3N-HMS-SP should be taken in the account of adsorption mechanism for real wastewater application.
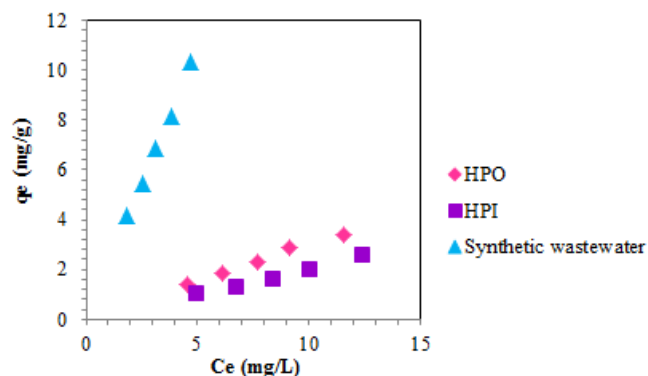
Figure 4. 12 CFA adsorption isotherms on 3N-HMS-SP of synthetic wastewater and NOM fraction in real wastewater

4.2.3.2 Effect of natural organic matter (NOM) in real wastewater

The presence of both hydrophilic and hydrophobic fraction of NOM is already proved the effects on the CFA adsorption efficiencies. In order to investigate the effect on active site competition between CFA and NOM, the adsorption capacities of both hydrophilic fraction and hydrophobic fraction of NOM are shown in the **figure 4.13**. From the obtained results, the adsorption of hydrophobic fraction was higher than the adsorption of hydrophilic fraction and did not decrease when the equilibrium concentration of CFA was increased. However, the adsorption of hydrophilic fraction was higher and continuingly decreases due to the increasing of CFA equilibrium concentration. Hence, it might be concluded that the presence of hydrophobic fraction of NOM on CFA adsorption efficiency was not stronger comparing with the hydrophilic NOM.
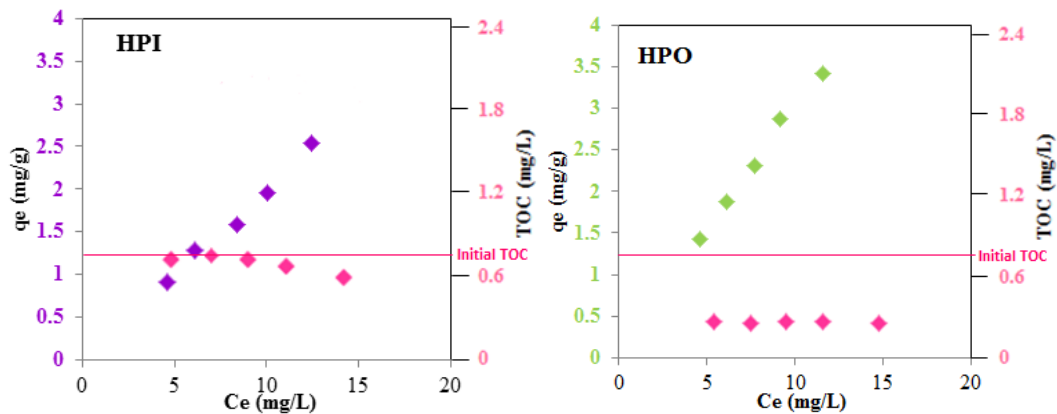
Figure 4. 13 CFA adsorption isotherms on 3N-HMS-SP of hydrophobic and hydrophilic NOM compare with total organic carbons (TOC)

4.3 High Gradient Magnetic Separation Filtration (HGMS filter)

The filtration column used in these experiments has internal diameter 1.9 cm, height 7 cm, the magnetic permanent, non-modified/ modified wire stainless 1.5 g. The adsorbent was selected to use in this section is HMS-SP. The parameters of stainless filter that shown in **Table 4.8**.

Table 4. 8 Parameters of stainless filter

Parameters	Values
Surface area (cm^2/g)	148.14
Density (g/cm^3)	7.8
Porosity of column	0.9321

The efficiency of stainless filter was calculated from equation (4.8);

$$Q = \frac{t \times F}{S} \qquad (4.8)$$

Where Q is breakthrough capacity (cm/cm^2), t is time at 10% of breakthrough (mins), F is flow rate (cm/min), and S is surface area (cm^2).

4.3.1 Effect of modified wire stainless

This experiment was used the stainless filter that were non-modified and modified wire stainless and designed breakthrough particle concentration at 10 % removal. **Figure 4.14** shows breakthrough curves of both modified and non-modified wire stainless filter at flow rate (velocity) 5 m/hr and particle concentration at 0.6 g/L. It was suggested that breakthrough time at breakthrough concentration (10%) was increased a little bit from 11 to 12 mins for non-modified and modified wire stainless filter, respectively. Calculated breakthrough information of both non-modified and modified wire stainless was concluded in **Table 4.9.** It can be seen that the parameter of weight of adsorbent in column/ weight of wire stainless (g/g) was not different, significantly. It mean that the retention efficiency of filter might not related to the hydrophobicity of the filter surface, hence, the hydraulic condition and concentration of particle should be the limiting factor for retention efficiency.
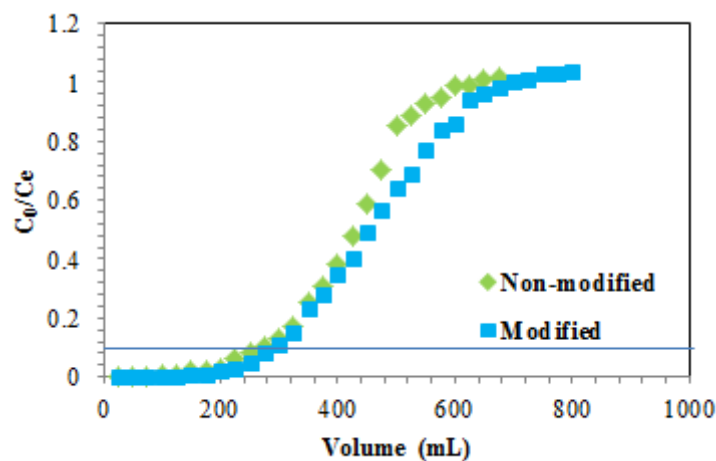
Figure 4. 14 Breakthrough curves of various modification of wire stainless

at flow rate 5 m/hr, particle concentration 0.6 g/L

Table 4. 9 The capacity of filtration column in various modification of wire stainless at porosity 0.9321, flow rate 5 m/hr, and particle concentration 0.6 g/L

Condition of wire stainless	Breakthrough time (mins)	Volume at breakthrough (cm^3)	Capacity of breakthrough (cm/cm^2)	Weights of adsorbent in column/weight of wire stainless (g/g)
Non-modification	11	275	0.4125	0.3908
Modification	12	300	0.4500	0.3914

4.3.2 Effect of flow rate

This experiment was designed breakthrough particle concentration at 10 % removal. The **Figure 4.15** shows breakthrough curves of three flow rates at particle concentration 0.6 g/L by using modified wire stainless. It can be seen that breakthrough time at breakthrough concentration was increased together with the increase of flow rate. High flow rate has more pressure to push the solution into separation column and it was decrease the breakthrough time to operate system (in **Table 4.10**; 92, 12, and 8 mins for 3, 5, and 7 m/hr, respectively). However, the flow rate (3m/hr) had the lowest stainless filter usage (weight of adsorbent in column/ weight of wire stainless (g/g)) at 0.3183 g/g (in **Table4.10**) which mean that the surface area of stainless filter was used less effectively compared with the higher flow rate.
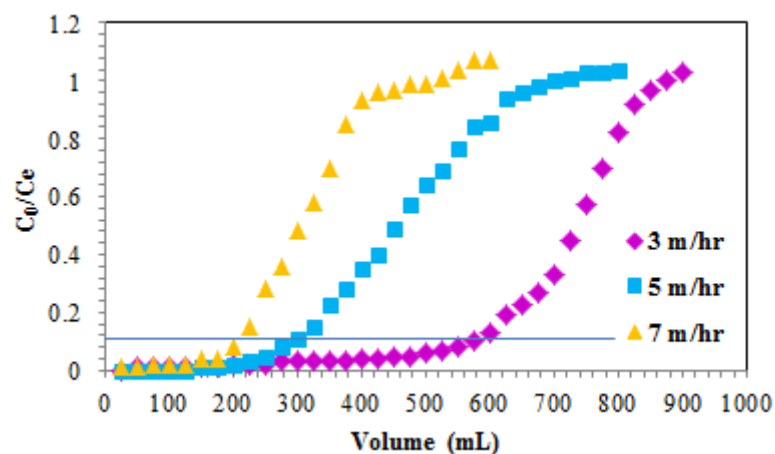
Figure 4. 15 Breakthrough curve of various flow rates

at particle concentration 0.6 g/L, modified wire stainless filter

Table 4. 10 The capacity of filtration column in various flow rates at porosity 0.9321, particle concentration 0.6 g/L, and modified wire stainless filter

Flow rate (m/hr)	Breakthrough time (mins)	Volume at breakthrough (cm^3)	Capacity of breakthrough (cm/cm^2)	Weights of adsorbent in column/weight of modified wire stainless (g/g)
3	92	575	2.0700	0.3183
5	12	300	0.4500	0.3914
7	8	200	0.4200	0.3933

4.3.3 Effect of particle concentration

The effect of particle concentration was determined by various the initial concentrations of adsorbent between 0.3 to 1 g/L at flow rate 5 m/hr and using modified wire stainless filter. It can be seen that high particle concentration had shorter time to operate the system; 16, 12, and 8 mins for 0.3, 0.6, and 1 g/L, respectively (**Figure 4.16).** The retention efficiency of high particle concentration

(1g/L) base on the weight of adsorbent in column/ weight stainless (g/g) (shown in
Table 4.11) indicated the highest efficiency at 0.6622 g/g.
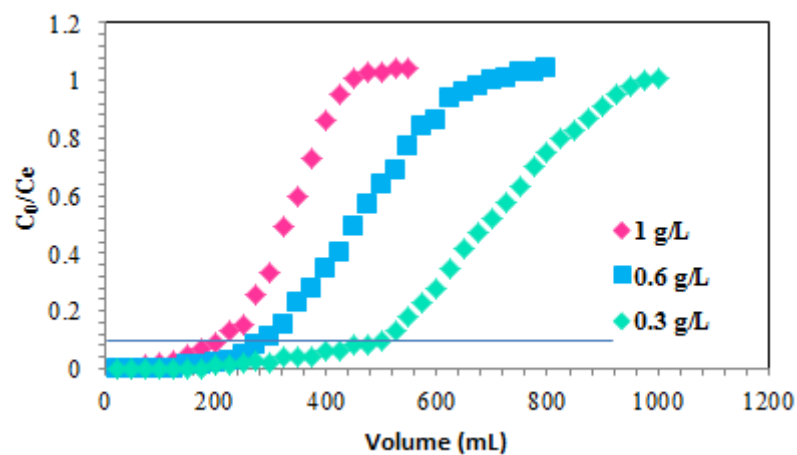
Figure 4. 16 Breakthrough curves of various particle concentrations

at flow rate 5 m/hr, modified wire stainless filter

Table 4. 11 The capacity of filtration column in various particle concentrations
at porosity 0.9321, flow rate 5 m/hr, and modified wire stainless filter

Particle concentration (g/L)	Breakthrough time (mins)	Volume at breakthrough (cm^3)	Capacity of breakthrough (cm/cm^2)	Weights of adsorbent in column/weight of modified wire stainless (g/g)
0.3	16	400	0.6000	0.1811
0.6	12	300	0.4500	0.3914
1	8	200	0.3000	0.6622

4.4 Iron release

After experiment of adsorption study, all of adsorbents were tested iron
release from adsorbents by Atomic Absorption Spectrometer (AAS) to evaluate the
property change during the adsorption experiment. The changes might effect to the
decrease of adsorption capacity and efficiency of magnetic separation. The results in

Table 4.12 showed that all of adsorbents were released iron (Fe) are less than 0.001 mg per g of adsorbent. Hence, it can be that all adsorbent did not change the content of iron, significantly during the adsorption experiment.

Table 4. 12 The total iron release under adsorption condition at 24 hr at phosphate buffer pH 7, IS 2 mM, and 25°C

Adsorbent	Concentration of Fe (mg/g)
HMS-SP	< 0.001
3N-HMS-SP	<0.001
M-HMS-SP	<0.001

CHAPTER V

CONCLUSION AND RECOMMENDATIONS

5.1 Conclusion

The aim of this research are to investigate the effect of functional group and pH on Clofibric acid (CFA) adsorption capacities and adsorption mechanism at high concentration, low concentration, and the effect of hydrophobic and hydrophilic NOM in real wastewater on CFA adsorption, including to investigate the effect of flow rate and particle concentration on separation of superparamagnetic mesoporous silicates from synthetic wastewater by hydrophobic modified High Gradient Magnetic Separation Filter (HGMS filter).

The superparamagnetic hexagonal mesoporous silicates were synthesized and coated by synthesized magnetite. The adsorbents were functionalized by post-grafting method with two functional groups such as amino and mercapto groups.

The physio-chemical properties were measured by XRD, FTIR, nitrogen adsorption, zeta potential, particle analyzer, and elemental analyzer. The results from characterizations were indicated that the functionalized adsorbents had the functional groups on surface adsorbents, and the synthesized adsorbents had particle diameter between 40-150 µm and diameter of pore size diameter between 50-150 Å, and pH_{pzc} of all adsorbents were used to explain in effect of pH on adsorption mechanism.

Adsorptions kinetic at high concentration, the experiment was conducted at initial concentration of 10 mg.L^{-1} and pH 7 controlled by phosphate buffer 2mM, 25°C. The data were matched with pseudo second order model. The equilibrium times of synthesized adsorbents are 6 hours while 2 hours for PAC. Adsorption isotherm were studied at initial concentration during 6-15 mg/L controlled by phosphate buffer 2 mM at pH 5, 7, and 9 (25°C). As the results, adsorption isotherms were fit with Freundlich model and the highest adsorption capacity follow in order; PAC>3N-HMS-SP>HMS-SP>M-HMS-SP, respectively. The effect of functional groups on CFA adsorption might relate to hydrogen bonding.

CFA adsorption at low concentration had a same trend of adsorption capacity at high concentration.

It was found that 3N-HMS-SP had higher CFA adsorption capacity in the presence of hydrophobic NOM than hydrophilic NOM. It might be caused by the interaction between hydrophilic NOM and hydrophilic amine functional group of 3N-HMS-SP, which can reduce the available active space for CFA.

The breakthrough times of HGMS filter were enhanced by decreasing of flow rate, and particle concentration. However, hydrophobic modified stainless could not enhance the retention of HMS-SP particle, significantly. The highest separation capacity on this research was conduct in flow rate higher than 5 m/hr of flow rate and 1 g/L of particle concentration. The retention efficiency was enhanced by increased separation column size and particle of adsorbent concentration.

5.2 Recommendations

5.2.1 Adsorption isotherm of CFA in all adsorbents at low concentration should be investigated due to it may be compare with other and get more information to describe the adsorption mechanism.

5.2.2 The stability of adsorbent structure and grafted functional groups on surface should be investigated and improved.

5.2.3 Adsorption removal process attached with superparamagnetic particle on HGMS filter should be investigated the over all efficiency.

REFERENCES

Abdullah, M. A., Chiang, L., Nadeem, M. (2009). Comparative evaluation of adsorption kinetics and isotherms of a natural product removal by Amberlite polymeric adsorbents. *Chemical engineering Journal, 146*(3), 370-376. doi: 10.1016/j.cej.2008.06.018

Baik, S. K., Ha, D. W., Ko, R. K. and Kwon, J. M. . (2010). Magnetic field and gradient analysis around matrix for HGMS. *Physica C: Superconductivity, 470*, 1831-1836.

Barnes, K. K., Kolpin, D. W., Furlong, E. T., Zaugg, S. D., Meyer, M. T. and Barber, L. B. . (2008). A national reconnaissance of pharmaceuticals and other organic wastewater contaminants in the United States--I) groundwater. *Science of the Total Environment, 402*(2-3), 192-200. doi: 10.1016/j.scitotenv.2008.04.028

Bhagat, S. D., Kim, Y. H. and Ahn, Y. S. . (2006). Room temperature synthesis of water repellent silica coatings by the dip coat technique. *Applied Surface Science, 253*, 2217-2221.

Boyd, G. R., Reemtsma, H., Grimm, D. A. and Mitra, S. . (2003). Pharmaceutical and personal care products (PPCPs) in surface and treated water of Loisiana, USA and Ontario. *Canada. Sci. Total Environ, 311*, 135-149.

Brandhof, E. a. M., M. . (2010). Fish embryo toxicity of carbamazepine, diclofenac and metoprolol. *Ecotoxicology and Environmental Safety, 73*, 1862–1866.

Bui, T. X., Choi, H. (2009). Adsorptive removal of selected pharmaceuticals by mesoporous silica SBA-15. *Journal of Hazardous Materials, 168*(2-3), 602-608.

Bui, T. X., Choi, H. (2010). Influence of ionic strength, anions, cations, and natural organic matter on the adsorption of pharmaceuticals to silica. *Chemosphere, 80*(7), 681-686. doi: 10.1016/j.chemosphere.2010.05.046

Buser, H. a. M.-l., M. D. . (1998). Occurrence of the Pharmaceutical Drug Clofibric Acid and the Herbicide Mecoprop in Various Swiss Lakes and in the North Sea. *Environment Science Technology, 32*, 188-192.

Cabrera-Lafaurie, W. A., Roman, F. R., Hernandez-Maldonado, A. J. (2012). Transition metal modified and partially calcined inorganic-organic pillared clays for the adsorption of salicylic acid, clofibric acid, carbamazepine, and caffeine from water. *J Colloid Interface Sci, 386*(1), 381-391. doi: 10.1016/j.jcis.2012.07.037

Ditsch, A., Lindenmann, S., Laibinis, P. E., Wang, D. I. C. and Hatton, T. A. (2005). High-gradient magnetic separation of magnetic nanoclusters. *Industial & Engineering Chemistry Research, 44*, 6824-6836.

Ferrari, B., Paxe´us, N., Giudice, R. L., Pollio, A. and Garrica, J. . (2003). Ecotoxicological impact of pharmaceuticals found in treated wastewaters: study of carbamazepine, clofibric acid, and diclofenac. *Ecotoxicology and Environmental Safety, 55*, 359-370. doi: 10.1016/S0147-6513(02)00082-9

Freundlich, H. M. F. (1906). Uber die adsorption in losungen. *Z. Phys. Chem, 57*, 385-471.

Gökmen, V. a. S., A. . (2002). Equilibrium and kinetic studies on the adsorption of dark colored compounds from apple juice using adsorbent resin. *Journal of Food Engineering, 53*, 221–227.

Heberer, T. (2002). Occurrence, fate, and removal of pharmaceutical residues in the aquatic environment: a review of recent research data. *Toxicology Letters, 131*, 5-17.

Ho, Y., Chiu, W., Wang, C. (2005). Regression analysis for the sorption isotherms of basic dyes on sugarcane dust. *Bioresource Technology, 96*, 1285-1291.

Hoffmann, F., Cornelius, M., Morell, J. M. F. . (2006). Silica-Based Mesoporous Organic-Inorganic Hybrid materials. *Angewandte Chemie International Edition, 45*, 3216-3251.

Hongsawat, P., Prarat, P., Ngamcharussrivichai, C. and Punyapalakul, P. . (2013). Adsorption of ciprofloxacin on surface functionalized superparamagnetic mesoporous silicatestess. *Desalination and Water Treatment*, 1-14. doi: 10.1080/19443994.2013.803795

Hua, J., An, P., Winter, J., Gallert, C. (2003). Elimination of COD, microorganisms and pharmaceuticals from sewage by trickling through sandy soil below leaking sewers. . *Water Research, 37*, 4395-4404.

Khan, M. A., Saeed, K., Abdullah, Ahmad, W., Mabood, F. and Rehman, M. . (2011). In vitro adsorption of drugs using modified sugarcane bagasse. . *Journal of Scientific & Industrial Research, 71*, 161-168.

Kimura, K., Iwase, T., Kita, S. and Watanabe, Y. . (2009). Influence of residual organic macromolecules produced in biological wastewater treatment processes on removal of pharmaceuticals by NF/RO membranes. *Water Research, 43*, 3751-3758.

Kummerer, K. (2009). A ntibiotics in the aquatic environment-A review-Part I. . *Chemosphere, 75*, 417-434. doi: 10.1016/j.chemosphere.2008.11.086

Kyzas, G. Z., Kostoglou, M., Lazaridis, N. K., Lambropoulou, D. A. and Bikiaris, D. N. (2013). Environmental friendly technology for the removal of pharmaceutical contaminants from wastewaters using modified chitosan adsorbents. *Chemical engineering Journal, 222*, 248-258. doi: 10.1016/j.cej.2013.02.048

Lin, H. Y., Chen, Y. W. (2005). Preparation of spherical hexagonal mesoporous silica. *Journal of Porous Materials, 12*, 95-105.

Liu, Z., Zhou, X., Chen, X., Dai, C., Zhang, J., Zhang, Y. (2013). Biosorption of clofibric acid and carbamazepine in aqueous solution by agricultural waste rice straw. *Journal of Environmental Sciences, 25*(12), 2384-2395. doi: 10.1016/s1001-0742(12)60324-6

Lortragool, W. (2009). *Coalescence process for treating lubricant oil in wastewater by with and without surface modified.* (Master), Chulalongkorn University, Chulalongkorn University.

Mall, I. D., Srivastava, V. C. and Agarwal, N. K. . (2006). Removal of Orange-G and Methyl Violet dyes by adsorption onto bagasse fly ash—kinetic study and equilibrium isotherm analyses. *Dyes and Pigments, 69*, 210-223.

Maria, C. A. S., Zhao, X. S., Kustedjo, A. T. and Qiao, S. Z. . (2004). Functionalization of large-pore mesoporous silicas with organosilanes by direct synthesis. *Microporous and Mesoporous Materials, 72*, 33-42.

Martı́nez-Carballo, E., González-Barreiro, C., Scharf, S. and Gans, O. . (2007). Environmental monitoring study of selected veterinary antibiotics in animal manure and soils in Austria. *Environmental Pollution, 148*, 570-579.

Matilainen, A., Gjessing, E. T., Lahtinen, T., Hed, L., Bhatnagarf, A. and Sillanpää, M. . (2011). An overview of the methods used in the characterisation of natural organic matter (NOM) in relation to drinking water treatment. *Chemosphere, 83*, 1431-1442.

Misuhashi, K., Yoshizaki, R., Okadab, H., Oharac, T. and Wada, H. . (2003). Purification of Endocrine Disrupter-polluted water using high temperature superconducting HGMS. *Physical Separation in Science and Engineering, 12*, 205-213.

Mompelat, S., Bot, B. L. and Thomas, O. (2009). Occurrence and fate of pharmaceutical products and by-products, from resource to drinking water. . *Environment International, 35*, 803-814.

Nadeema, M., Mahmooda, A., Shahidb, S. A., Shahc, S. S., Khalidd, A. M. and McKaye, G. . (2006). Sorption of lead from aqueous solution by chemically modified carbon adsorbents. *Journal of Hazardous Materials, 138*, 604-613.

Nie, Y., Deng, S., Wang, B., Huang, J. and Yu, G. . (2013). Removal of clofibric acid from aqueous solution by polyethylenimine-modified chitosan beads. . *Frontiers of Environmental Science & Engineering.*

Nunes, B., Gaioc, A.R., Carvalho, F. and Guilhermino, L. . (2008). Behaviour and biomarkers of oxidative stress in Gambusia holbrooki after acute exposure to widely used pharmaceuticals and a detergent. *Ecotoxicology and Environmental Safety, 71*(2), 341-354. doi: 10.1016/j.ecoenv.2007.12.006

Oosterhuis, M., Sacher, F. and Laak, T. L. . (2013). Prediction of concentration levels of metformin and other high consumption pharmaceuticals in wastewater and regional surface water based on sales data. *Science of the Total Environment, 442*, 380-388. doi: 10.1016/j.scitotenv.2012.10.046

Pinnavaia, P., Tanev, T., Thomas, J. (1995). Neutral templating route to mesoporous molecular sieves. *Science, 267*, 865-867.

Punyapalakul, P., Satochi, T. (2004). Effect of organic grafting modification of hexagonal mesoporous silicate on haloacetic acid removal. *Environment Engineering Research, 41*.

Reddersen, K., Heberer, T. and Dunnbier, Uwe. . (2002). Identification and significance of phenazone drugs and their metabolites in ground- and drinking water. . *Chemosphere, 49*, 539-544.

Rosal, R., Gonzalo, M. S., Boltes, K., Leton, P., Vaquero, J. J., Garcia-Calvo, E. (2009). Identification of intermediates and assessment of ecotoxicity in the oxidation products generated during the ozonation of clofibric acid. *J Hazard Mater, 172*(2-3), 1061-1068. doi: 10.1016/j.jhazmat.2009.07.110

Ruangtrakul, W. (2010). *Appilcation of superparamagnetic mesoporous silicatestes on naproxen removal.* (Master), Chulalongkorn University, Chulalongkorn University.

Salgado, R., Oehmen, A., Carvalho, G., Noronha, J. P. and Reis, M. A. M. . (2012). Biodegradation of clofibric acid and identification of its metabolites. . *Journal of Hazardous Materials, 241-242*, 182-189. doi: 10.1016/j.jhazmat.2012.09.029

Samuel, D. F. a. O., M. A. . (1987). *Adsorption processes for water treatment* (2 ed.). London: Butterworths Publishers.

Sato, R. T., Kerschl, P., Fukunaga, H., Kawazoe, Y., Shintani, A., Grössinger R. (2004). Effect of magnetostatic interaction on magnetic properties of mixed powders: computer simulation and experimental results *Journal of Magnetism and Magnetic Materials, 272–276*, E497–E498.

Sing, K. S. W. (1982). Reporting physisorption data for gas/solid systems with special reference to determination of surface area and porosity. *Pure & Appl. Chem, 54*, 2201-2218.

Skadsen, J. M., Rice, B. L., and Meyering, D. J. (2004). The occurrence and fate of pharmaceuticals, personal care products and endocrine disrupting compounds in a municipal water use cycle: a case study in the city of Ann Arbor. *City of Ann Arbor, Water Utilities and Fleis & VandenBrink Engineering, Inc.*

Stein, A., M, B. J. and C, S. R. . (2000). Hybrid Inorganic-Organic Mesoporous Silicates-Nanoscopic Reactors Coming of Age. *Advanced Materials, 12*, 1403-1419.

Tanev, P. T., Chibwe, M. and Pinnavaia, T. J. . (1994). Titanium-containing mesoporous molecular sieves for catalytic oxidation of aromatic compounds. *Nature, 368*, 321-323.

Ternes, T. A. (1998). Occurrence of drugs in German sewage treatment plants and rivers. *Water Research, 32*, 3245-3260.

Tian, G., Gomersall, C. D., Wong, A., Leung, P., Choi, G., Joynt, G. M., Tan, P. and Lipmana, J. . (2006). Effect of drug concentration on adsorption of levofloxacin by polyacrylonitrile haemofilters. . *International Journal of Antimicrobial Agents, 28*, 147-150. doi: 10.1016/j.ijantimicag.2006.03.025

Tian, H., Li, J., Shen, Q., Wang, H., Hao, Z., Zou, L., & Hu, Q. (2009). Using shell-tunable mesoporous Fe3O4@HMS and magnetic separation to remove DDT from aqueous media. *Journal of Hazardous Materials, 171*(1-3), 459-464.

Tian, H., Li, J., Shen, Q., Wang, H., Hao, Z., Zou, L. and Hu, Q. (2009). Using shell-tunable mesoporous Fe_3O_4@HMS and magnetic separation to remove DDT from aqueous media. . *Journal of Hazardous Materials, 171*, 459-464.

Wang, Y., Ren, J., Liu, X., Wang, Y., Guo, Y., Guo Y. and Lu, G. . (2008). Facile synthesis of ordered magnetic mesoporous Fe_2O_3/SiO_2 nanocomposites with diverse mesostructures. *Journal of Colloid and Interface Science, 326*, 158-165.

Yousef, R. I., El-Eswed, B. and Al-Muhtaseb, A. (2011). Adsorption characteristics of natural zeolites as solid adsorbents for phenol removal from aqueous solutions: Kinetics, mechanism, and thermodynamics studies. *Chemical engineering Journal, 171*, 1143-1149.

Zhao D., F. J., Huo Q., Melosh N., Fredroickson G.H., Chmelka B.F. and G.D., S. . (1998). Triblock copolymer syntheses of mesoporous silica with periodic 50-300 angstrom pores. *Science, 279*, 548-552.

Ziylan, A. a. I., N. H. . (2013). Ozonation-based advanced oxidation for pre-treatment of water with residuals of anti-inflammatory medication. *Chemical engineering Journal, 220*, 151-160. doi: 10.1016/j.cej.2012.12.071

Zuccato, E., Calamari, D., Natangelo, M. and Fanelli, R. . (2000). Presence of therapeutic drugs in the environment. *The Lancet, 355*, 1789-1790. doi: 10.1016/S0140-6736(00)02270-4

APPENDIX

APPENDIX A

Appendix A: Characterization of synthesis adsorbents

Table A-1: Data from calculation of surface charge density of HMS-SP and functionalized HMS-SP

pH	Surface charge density (C/g)		
	HMS-SP	3N-HMS-SP	M-HMS-SP
3.02	0.0213	0.0482	0.0391
4.03	0.0110	0.0399	0.0340
4.81	0.0069	0.0337	0.0174
5.96	-0.0044	0.0224	0.0060
7.19	-0.0045	0.0126	-0.0057
7.96	-0.0060	0.0226	-0.0069
9.03	-0.0118	0.0095	-0.0246
9.93	-0.0163	-0.0291	-0.0762

APPENDIX B

Appendix B: Adsorption at high concentration

Table B-1: Kinetic data of HMS-SP, functionalized HMS-SP, and PAC at initial concentration 10 mg/L, pH7, and IS 2mM

Time (min)	Concentration (mg/L)			
	HMS-SP	3N-HMS-SP	M-HMS-SP	PAC
0.5	-	-	-	6.73
1	3.24	3.93	0.08	7.10
3	-	-	-	8.38
5	3.78	4.91	0.12	8.55
7	-	-	-	8.86
10	4.33	5.38	0.15	8.94
12	-	-	-	8.97
15	-	-	-	9.00
20	4.74	6.01	0.18	9.04
25	-	-	-	9.07
30	5.11	6.60	0.21	9.09
40	-	-	-	9.15
60	5.41	6.85	0.26	9.27
90	-	-	-	9.35
120	5.83	7.05	0.28	9.36
150	-	-	-	9.37
180	-	-	-	9.42
240	6.01	7.11	0.34	9.43
260	6.16	7.14	0.36	9.44
280	6.36	7.16	0.37	9.44
300	6.43	7.19	0.38	6.73
320	6.52	7.20	0.39	7.10
340	6.59	7.26	0.40	8.38
360	6.61	7.40	0.41	8.55
480	6.65	7.52	0.42	8.86

Table B-2: Isotherm data of HMS-SP at initial concentration of CFA during 6-15 mg/L controlled by phosphate buffer 2 mM at pH 5, 7, and 9, 25℃

Initial concentration (mg/L)	pH 5		pH 7		pH 9	
	Ce (mg/L)	qe (mg/g)	Ce (mg/L)	qe (mg/g)	Ce (mg/L)	qe (mg/g)
6	2.55	3.44	2.28	3.71	2.73	3.26
8	3.44	4.55	3.33	4.66	3.54	4.45
10	3.60	6.39	3.93	6.06	4.08	5.91
12	4.19	7.80	4.64	7.35	4.82	7.17
15	5.10	9.89	5.58	9.41	5.15	9.84

Table B-3: Isotherm data of 3N-HMS-SP at initial concentration of CFA during 6-15 mg/L controlled by phosphate buffer 2 mM at pH 5, 7, and 9, 25℃

Initial concentration (mg/L)	pH 5		pH 7		pH 9	
	Ce (mg/L)	qe (mg/g)	Ce (mg/L)	qe (mg/g)	Ce (mg/L)	qe (mg/g)
6	2.09	3.90	1.83	4.16	2.24	3.75
8	2.57	5.42	2.51	5.48	2.69	5.30
10	2.94	7.05	3.10	6.89	3.15	6.84
12	3.36	8.63	3.82	8.17	4.07	7.92
15	3.97	11.02	4.68	10.31	5.14	9.85

Table B-4: Isotherm data of M-HMS-SP at initial concentration of CFA during 6-15 mg/L controlled by phosphate buffer 2 mM at pH 5, 7, and 9, 25℃

Initial concentration (mg/L)	pH 5		pH 7		pH 9	
	Ce (mg/L)	qe (mg/g)	Ce (mg/L)	qe (mg/g)	Ce (mg/L)	qe (mg/g)
6	5.63	0.36	5.59	0.40	5.69	0.30
8	7.54	0.45	7.53	0.46	7.62	0.37
10	9.48	0.51	9.46	0.53	9.53	0.46
12	11.34	0.65	11.38	0.61	11.38	0.61
15	14.17	0.82	14.31	0.68	14.26	0.73

Table B-5: Isotherm data of PAC at initial concentration of CFA during 6-15 mg/L controlled by phosphate buffer 2 mM at pH 5, 7, and 9, 25°C

Initial concentration (mg/L)	pH 5		pH 7		pH 9	
	Ce (mg/L)	qe (mg/g)	Ce (mg/L)	qe (mg/g)	Ce (mg/L)	qe (mg/g)
6	0.09	5.90	0.21	5.78	0.66	5.33
8	0.13	7.86	0.36	7.63	0.96	7.03
10	0.18	9.81	0.42	9.57	1.20	8.79
12	0.22	11.77	0.51	11.48	1.40	10.59
15	0.29	14.70	0.61	14.38	1.62	13.37
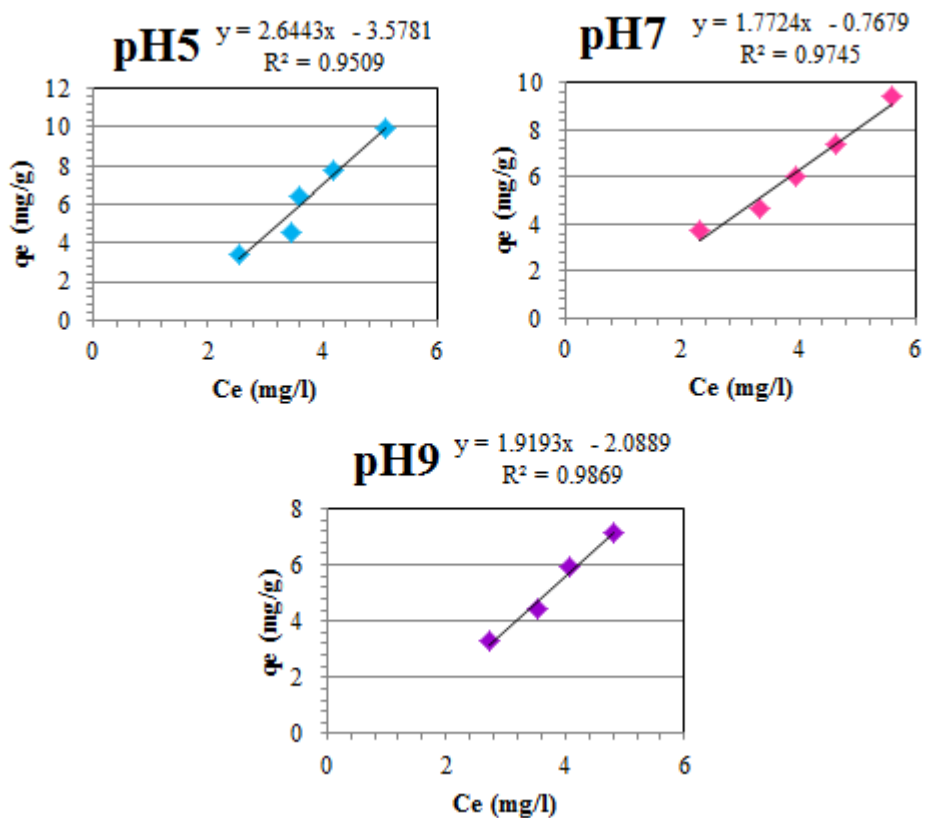
Figure B-1 Linear isotherm of HMS-SP
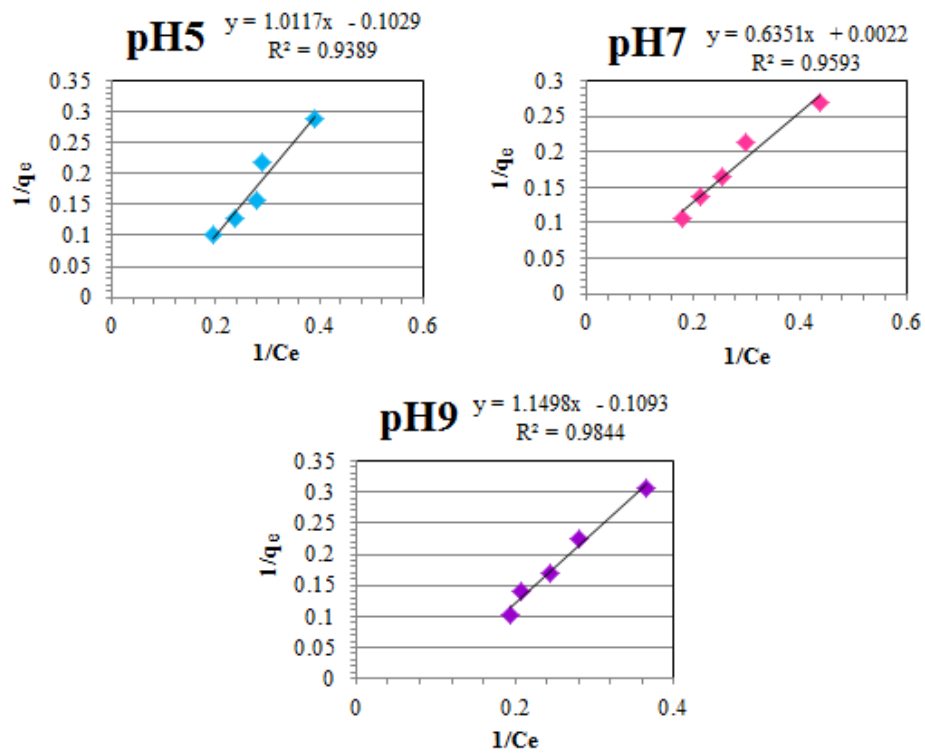
Figure B-2 Langmuir isotherm of HMS-SP
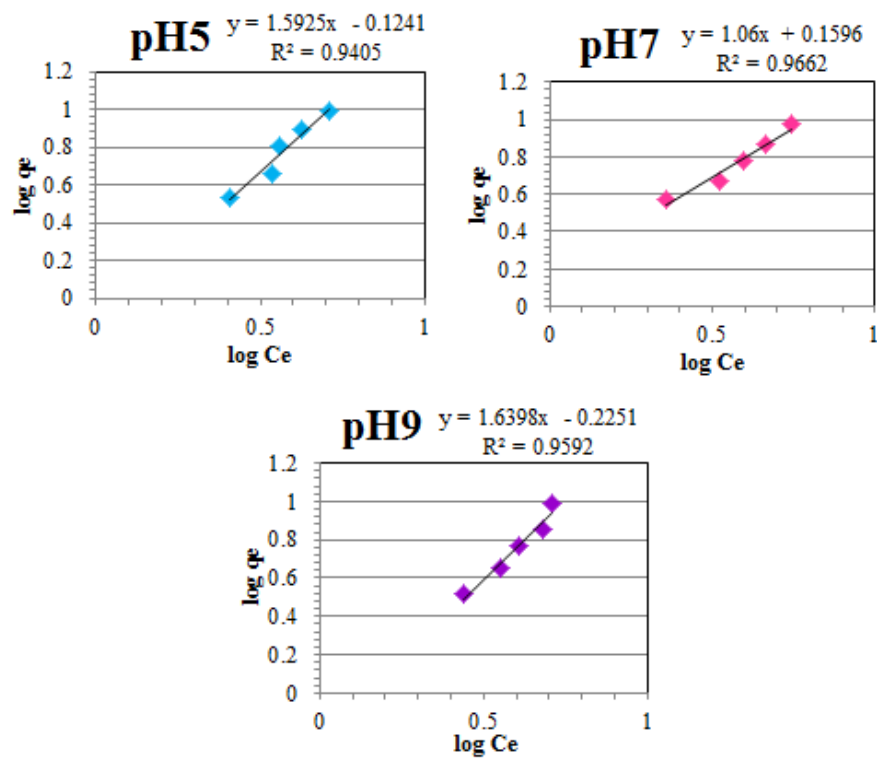
Figure B-3 Freundlich isotherm of HMS-SP
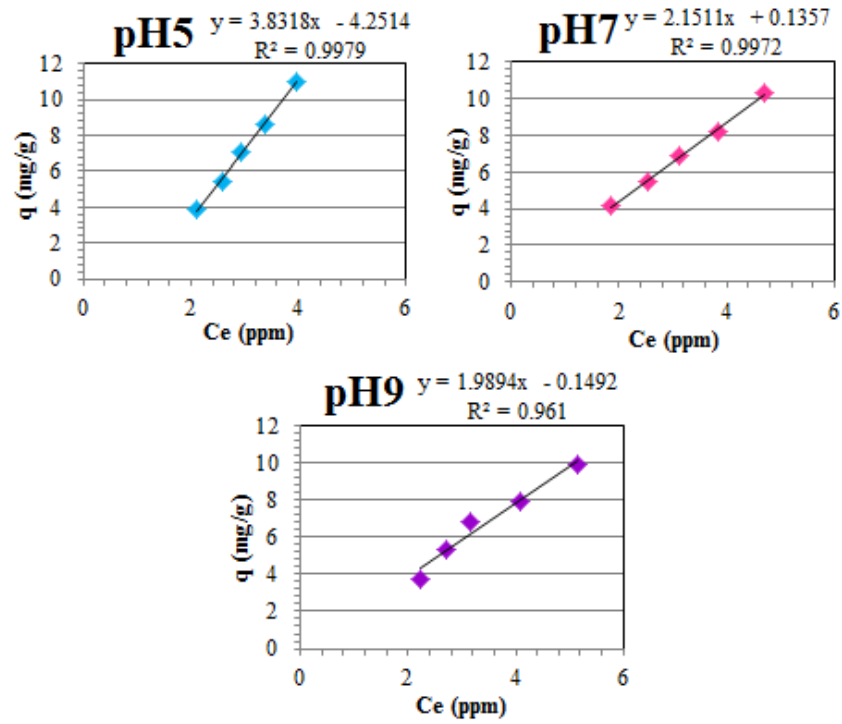
Figure B-4 Linear isotherm of 3N-HMS-SP
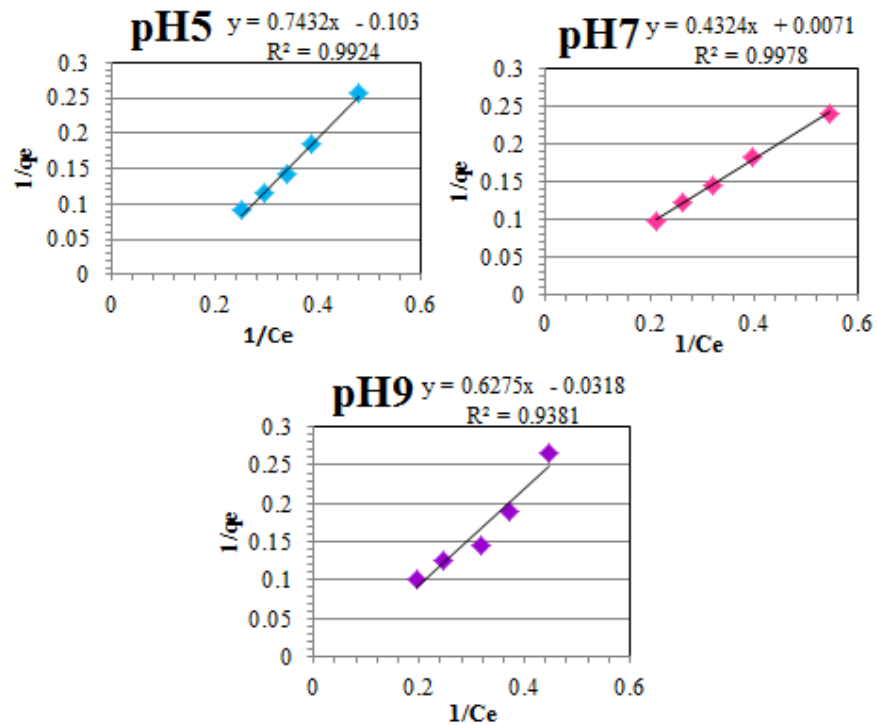
Figure B-5 Langmuir isotherm of 3N-HMS-SP
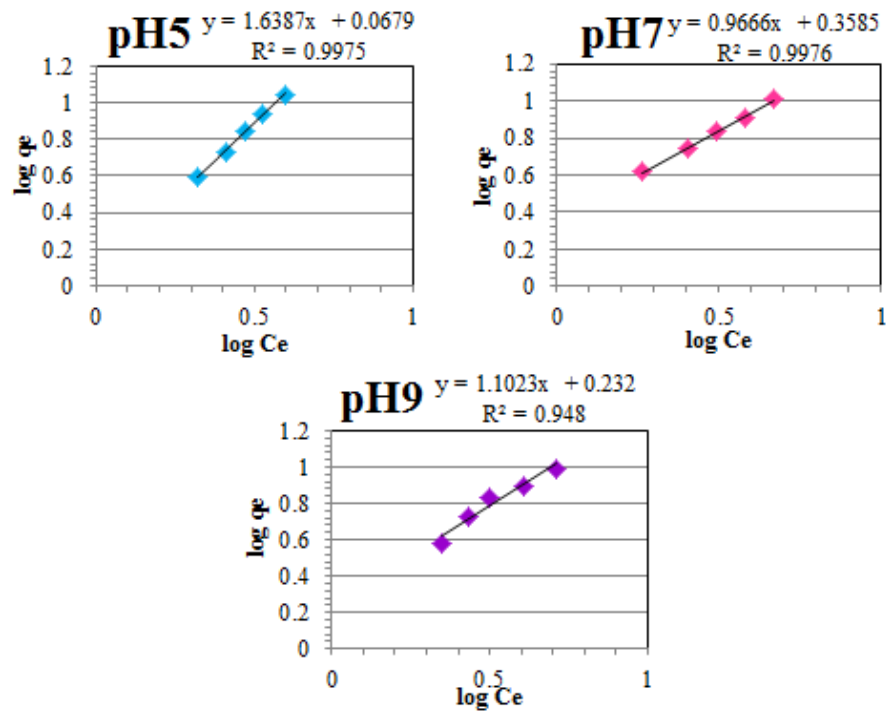
Figure B-6 Freundlich isotherm of HMS-SP
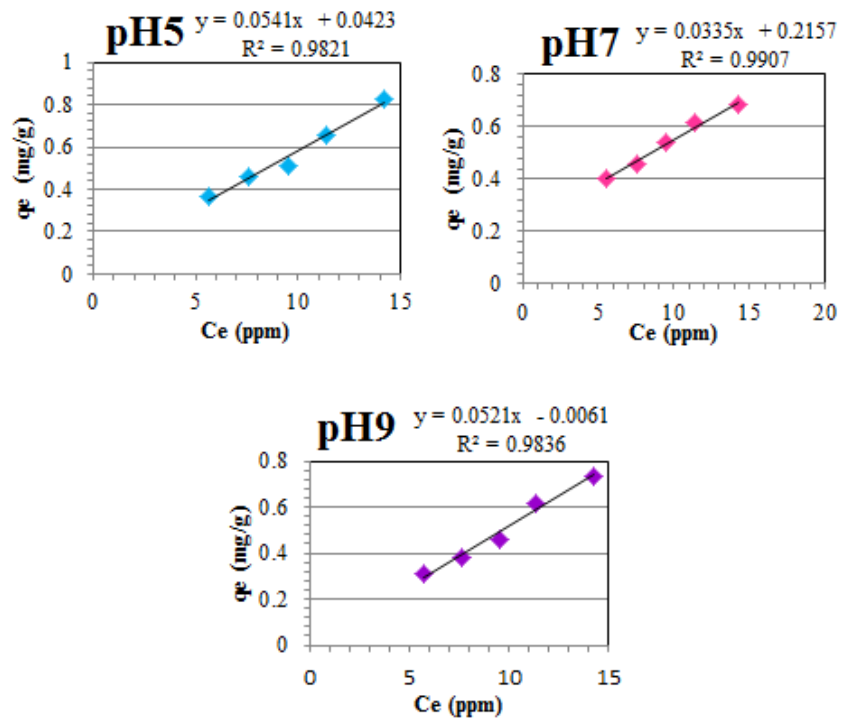
Figure B-7 Linear isotherm of M-HMS-SP
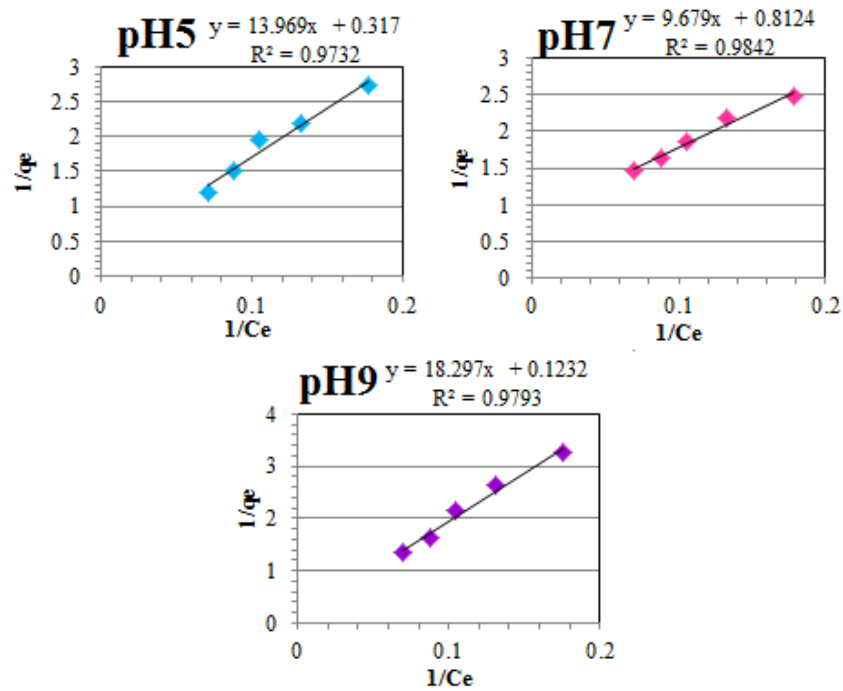
Figure B-8 Langmuir isotherm of M-HMS-SP
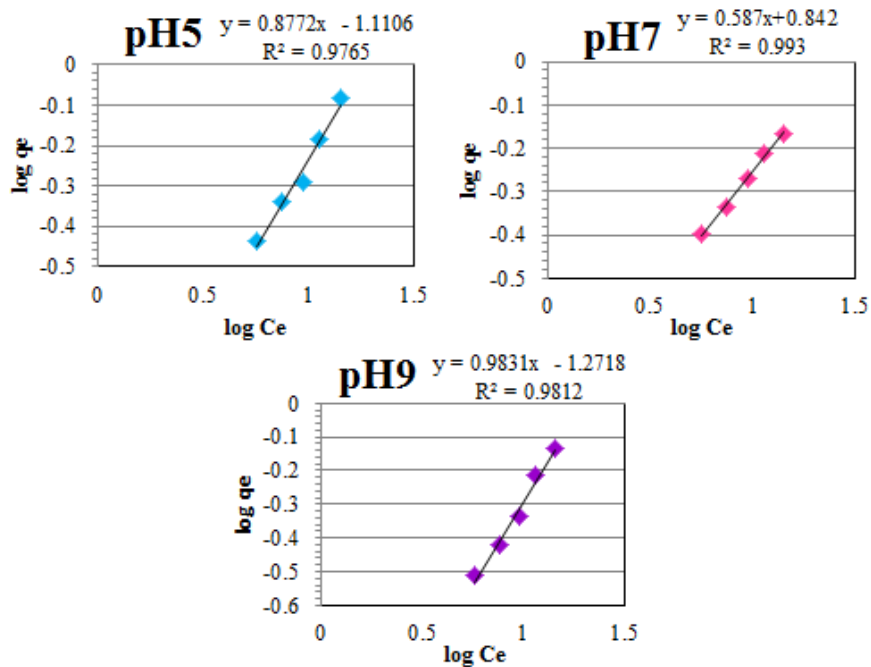
Figure B-9 Freundlich isotherm of M-HMS-SP
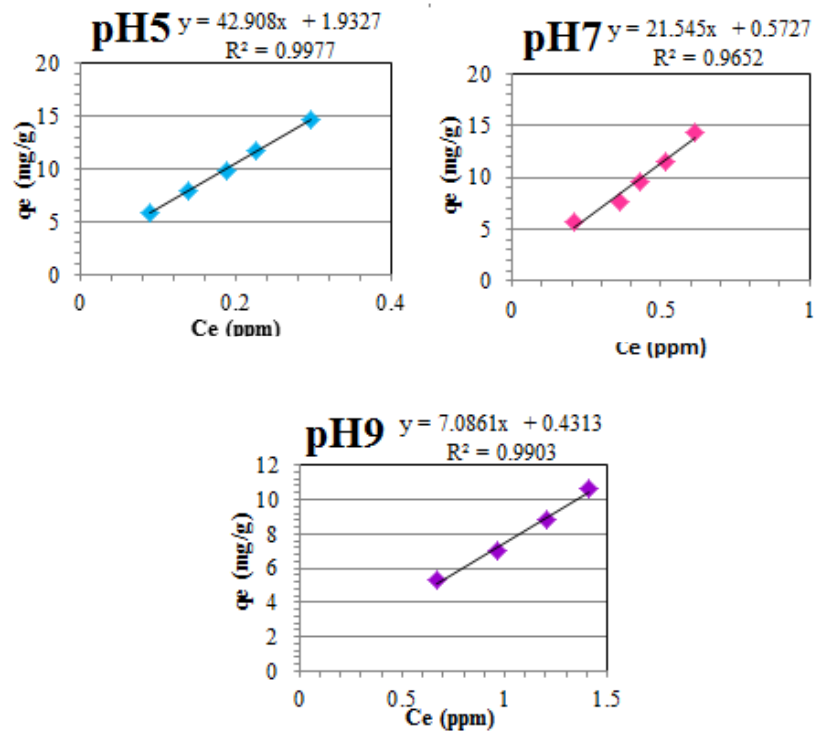
Figure B-10 Linear isotherm of PAC
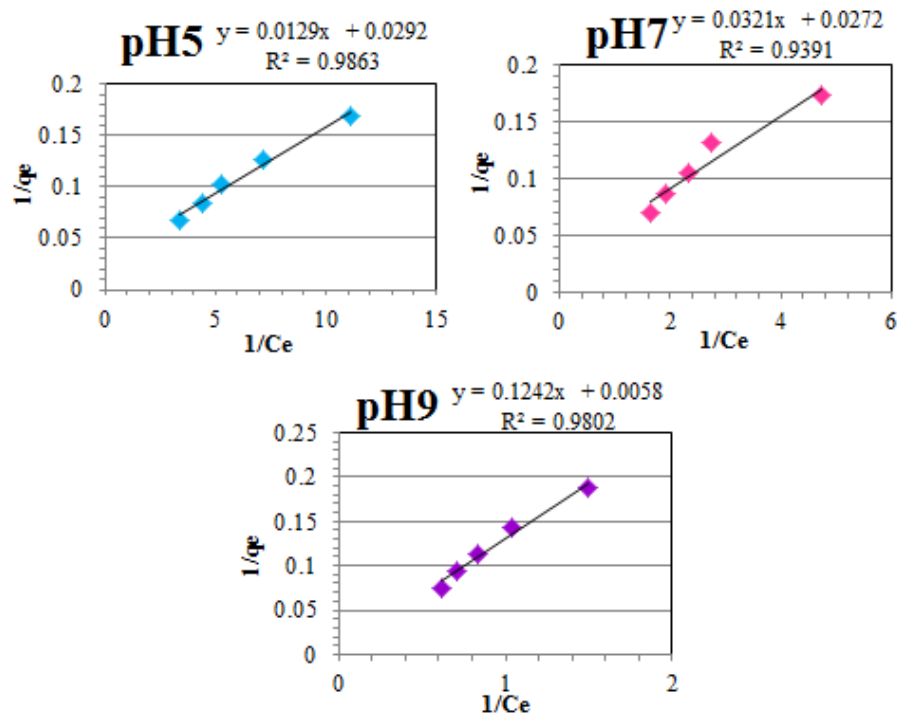
Figure B-11 Langmuir isotherm of PAC
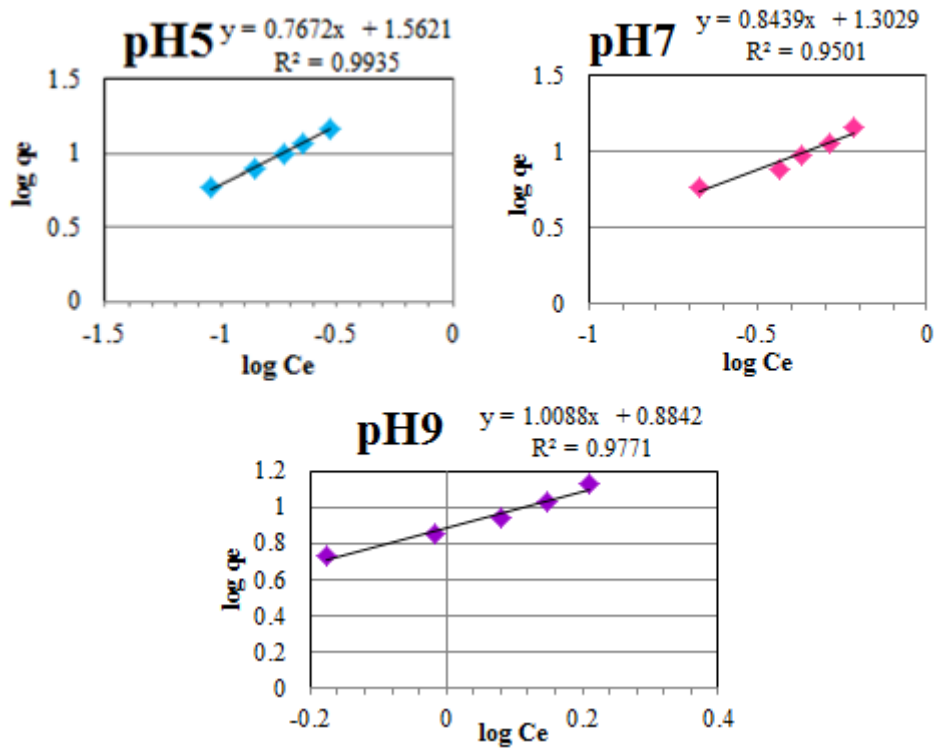
Figure B-12 Freundlich isotherm of PAC

Table B-6: Intraparticle diffusion data of HMS-SP, functionalized HMS-SP, and PAC

HMS-SP		3N-HMS-SP		M-HMS-SP		PAC	
Time $(h^{1/2})$	q (mg/g)	Time $(h^{1/2})$	q (mg/g)	Time $(h^{1/2})$	q (mg/g)	Time $(h^{1/2})$	q (mg/g)
0.12	3.24	0.12	3.93	0.12	0.08	0.09	6.73
0.28	3.78	0.28	4.91	0.28	0.12	0.12	7.10
0.40	4.33	0.40	5.38	0.40	0.15	0.22	8.38
0.57	4.74	0.57	6.01	0.57	0.18	0.28	8.55
0.70	5.11	0.70	6.60	0.70	0.21	0.34	8.86
1.00	5.41	1.00	6.85	1.00	0.26	0.40	8.94
1.41	5.83	1.41	7.05	1.41	0.28	0.44	8.97
1.73	5.97	1.73	7.08	1.73	0.31	0.50	9.00
2.00	6.01	2.00	7.11	2.00	0.34	0.57	9.04
2.08	6.16	2.08	7.14	2.08	0.36	0.64	9.07
2.16	6.36	2.16	7.16	2.16	0.37	0.70	9.09
2.23	6.43	2.23	7.19	2.23	0.38	0.81	9.15
2.30	6.52	2.30	7.20	2.30	0.39	1.00	9.27
2.38	6.59	2.38	7.26	2.38	0.40	1.22	9.35
2.44	6.61	2.44	7.40	2.44	0.41	1.41	9.36
2.82	6.65	2.82	7.52	2.82	0.42	1.58	9.37
3.46	6.71	3.46	7.54	3.46	0.43	1.73	9.42
-	-	-	-	-	-	2.00	9.43
-	-	-	-	-	-	2.44	9.44
-	-	-	-	-	-	2.82	9.44

Table B-7: Standard curve data of CFA

pH 5		pH 7		pH 9	
Concentration (mg/L)	Area	Concentration (mg/L)	Area	Concentration (mg/L)	Area
0.5	248	0.5	530	0.5	385
1	392	1	661	1	417
8	1579	8	2163	8	1996
10	1899	10	2525	10	2455

pH5 $y = 171.86x + 191.66$
$R^2 = 0.9991$
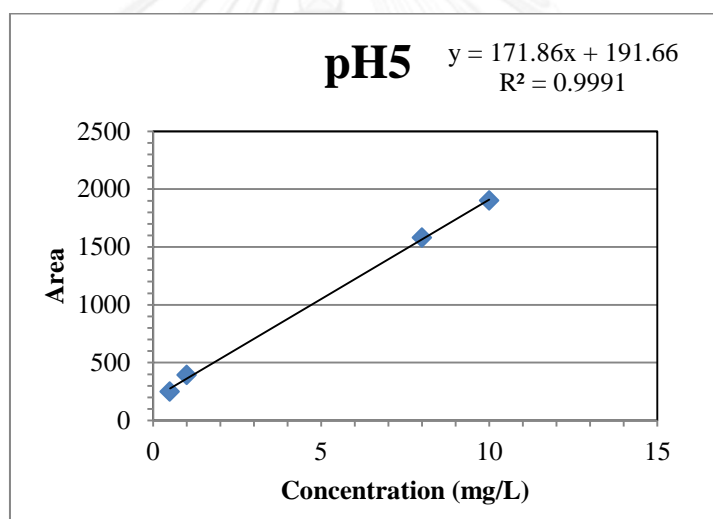
Figure B-13 Standard curve of CFA at pH 5
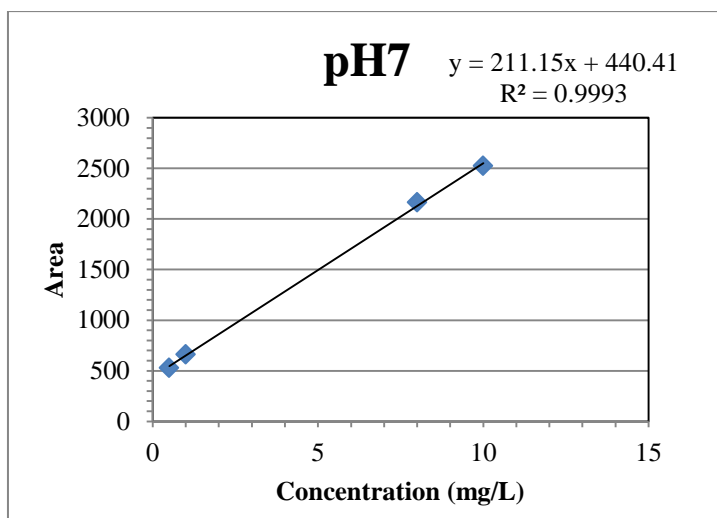
Figure B-14 Standard curve of CFA at pH 7
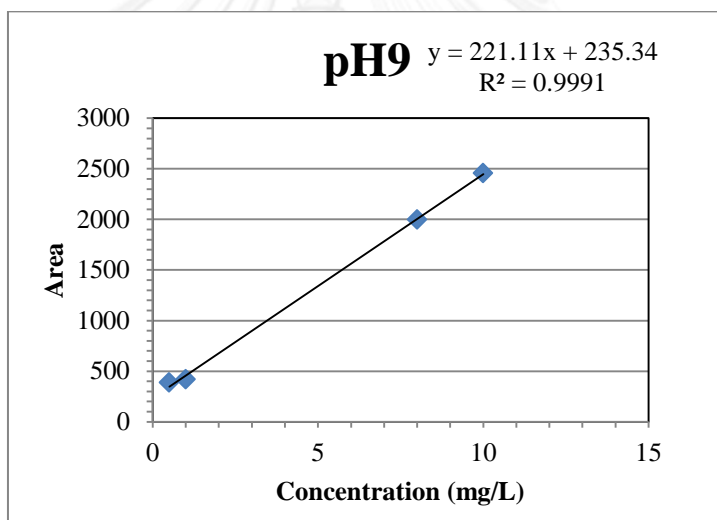
Figure B-15 Standard curve of CFA at pH 9

Appendix C

Appendix C: Adsorption at low concentration

Table C-1: The recovery percentage and the recovery standard deviation percentage of solid phase extraction (SPE)

The recovery percentage	%SD	%RSD
95.33	2.49	2.62

Table C-2: Isotherm data of 3N-HMS-SP at initial concentration of CFA during 50-250 µg/L controlled by phosphate buffer 2 mM at pH 7, and 25°C

Initial concentration (µg/L)	pH 7	
	Ce (µg/L)	qe (µg/g)
50	15.52	34.47
100	28.86	71.13
150	43.03	106.96
200	65.05	134.94
250	79.78	170.21

Table C-3: Standard curve data of CFA

pH 7	
Concentration (µg/L)	Area
50	219
150	352
250	486
300	547
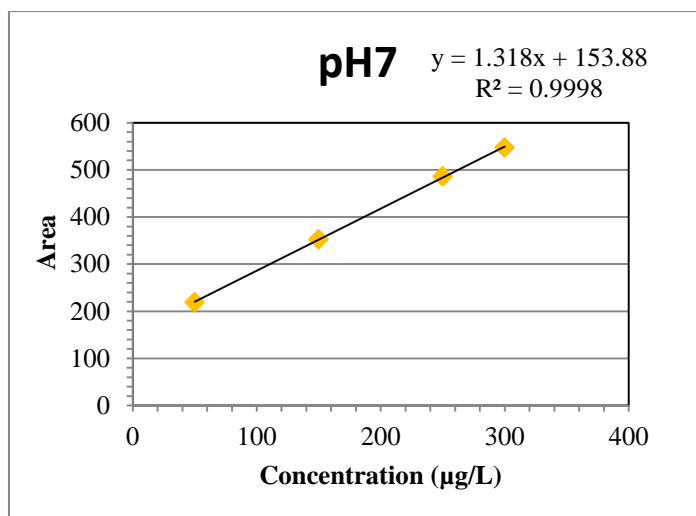
Figure C-1 Standard curve of CFA at pH 7

Appendix D

Appendix D: Adsorption of real wastewater

Table D-1: Isotherm data of 3N-HMS-SP in hydrophobic and hydrophilic NOM fractions at initial concentration of CFA during 6-15 mg/L controlled by phosphate buffer 2 mM at pH 7, 25°C

Initial concentration (mg/L)	Hydrophobic NOM		Hydrophilic NOM	
	C_e (mg/L)	q_e (mg/g)	C_e (mg/L)	q_e (mg/g)
6	4.57	1.42	5.01	0.98
8	6.12	1.87	6.74	1.25
10	7.69	2.30	8.41	1.58
12	9.13	2.86	10.04	1.95
15	11.58	3.41	12.46	2.53

Table D-2: Standard curve data of CFA

Hydrophobic NOM		Hydrophilic NOM	
Concentration (mg/L)	Area	Concentration (mg/L)	Area
1	496	1	359
6	1954	6	2159
8	2474	8	2778
15	4327	15	5148

Hydrophobic NOM $y = 272.62x + 268.11$ $R^2 = 0.9992$
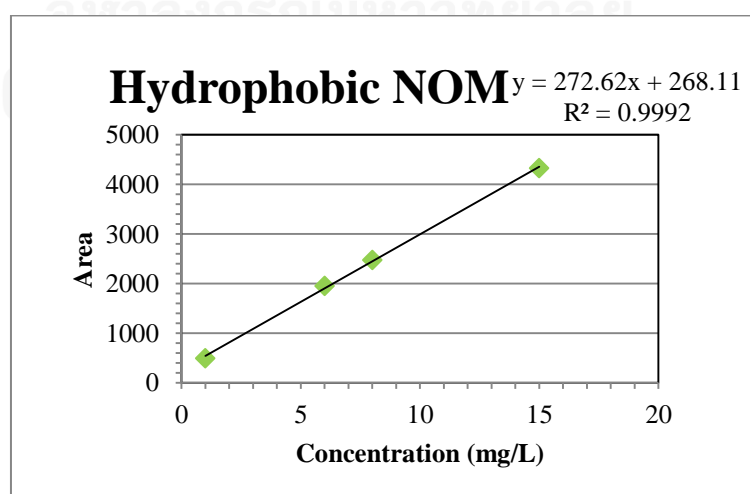
Figure D-1 Standard curve of CFA at hydrophobic NOM fraction
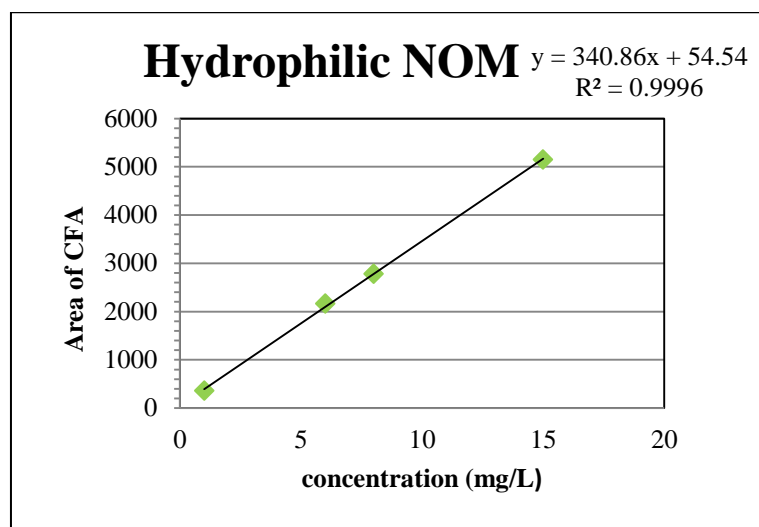
Figure D-2 Standard curve of CFA at hydrophilic NOM fraction

Table D-3: TOC data of 3N-HMS-SP in hydrophobic and hydrophilic NOM fractions at initial concentration of CFA during 6-15 mg/L controlled by phosphate buffer 2 mM at pH 7, 25°C

Hydrophobic NOM		Hydrophilic NOM	
C_0 of CFA (mg/L)	TOC (mg/L)	C_0 of CFA (mg/L)	TOC (mg/L)
6	1.42	6	2.19
8	1.87	8	2.17
10	2.30	10	2.14
12	2.86	12	2.09
15	3.41	15	2.01

Appendix E

Appendix E: Separation of adsorbent

Table E-1: Breakthrough data of variation non-modified stainless filter and modified stainless filter at flow rate 5 m/hr, particle concentration 0.6 g/L, porosity = 0.9321

Non-modified stainless filter		Modified stainless filter	
Volume (mL)	C/C_0	Volume (mL)	C/C_0
25	0	25	0
50	0	50	0
75	0	75	0
100	0.01	100	0
125	0.01	125	0
150	0.02	150	0.01
175	0.02	175	0.01
200	0.03	200	0.02
225	0.06	225	0.03
250	0.08	250	0.05
275	0.1	275	0.08
300	0.13	300	0.11
325	0.17	325	0.15
350	0.25	350	0.23
375	0.31	375	0.28
400	0.38	400	0.35
425	0.48	425	0.4
450	0.59	450	0.49
475	0.70	475	0.57
500	0.85	500	0.64
525	0.89	525	0.69
550	0.93	550	0.77
575	0.95	575	0.84
600	0.99	600	0.86
625	0.99	625	0.94
650	1.01	650	0.96
675	1.02	675	0.98
Stop		700	1.00
-	-	725	1.01
-	-	750	1.03
-	-	775	1.03
-	-	800	1.04

Table E-2: Breakthrough data of variation flow rate at modified stainless filter, particle concentration 0.6 g/L, porosity = 0.9321

3 m/hr		5 m/hr		7 m/hr	
Time (min)	C/C_0	Time (min)	C/C_0	Time (min)	C/C_0
1	0	1	0	1	0.01
2	0	2	0	2	0.01
3	0	3	0	3	0.02
4	0	4	0	4	0.02
5	0.01	5	0	5	0.02
6	0.01	6	0.01	6	0.04
7	0.01	7	0.01	7	0.04
8	0.01	8	0.02	8	0.08
9	0.01	9	0.03	9	0.15
10	0.01	10	0.05	10	0.28
11	0.01	11	0.08	11	0.36
12	0.01	12	0.11	12	0.48
13	0.01	13	0.15	13	0.58
14	0.01	14	0.23	14	0.70
15	0.01	15	0.28	15	0.85
16	0.01	16	0.35	16	0.93
17	0.01	17	0.4	17	0.96
18	0.01	18	0.49	18	0.97
19	0.01	19	0.57	19	0.99
20	0.01	20	0.64	20	0.99
21	0.01	21	0.69	21	1.01
22	0.01	22	0.77	22	1.04
23	0.01	23	0.84	23	1.07
24	0.01	24	0.86	24	1.07
25	0.01	25	0.94	25	1.08
26	0.01	26	0.96	Stop	
27	0.01	27	0.98	-	-
28	0.01	28	1.00	-	-
29	0.01	29	1.01	-	-
30	0.01	30	1.03	-	-
31	0.01	31	1.03	-	-
32	0.02	32	1.04	-	-
33	0.02	Stop		-	-
34	0.02	-	-	-	-
35	0.02	-	-	-	-
36	0.02	-	-	-	-
37	0.02	-	-	-	-

Table E-2 (continued): Breakthrough data of variation flow rate at modified stainless

filter, particle concentration 0.6 g/L, porosity = 0.9321

3 m/hr		5 m/hr		7 m/hr	
Time (min)	C/C_0	Time (min)	C/C_0	Time (min)	C/C_0
38	0.02	-	-	-	-
39	0.02	-	-	-	-
40	0.02	-	-	-	-
41	0.02	-	-	-	-
42	0.02	-	-	-	-
43	0.02	-	-	-	-
44	0.03	-	-	-	-
45	0.03	-	-	-	-
46	0.03	-	-	-	-
47	0.03	-	-	-	-
48	0.03	-	-	-	-
49	0.03	-	-	-	-
50	0.03	-	-	-	-
51	0.03	-	-	-	-
52	0.03	-	-	-	-
53	0.03	-	-	-	-
54	0.03	-	-	-	-
55	0.03	-	-	-	-
56	0.03	-	-	-	-
57	0.03	-	-	-	-
58	0.03	-	-	-	-
59	0.03	-	-	-	-
60	0.03	-	-	-	-
61	0.04	-	-	-	-
62	0.04	-	-	-	-
63	0.04	-	-	-	-
64	0.04	-	-	-	-
65	0.04	-	-	-	-
66	0.04	-	-	-	-
67	0.04	-	-	-	-
68	0.04	-	-	-	-
69	0.04	-	-	-	-
70	0.05	-	-	-	-

Table E-2 (continued): Breakthrough data of variation flow rate at modified stainless filter, particle concentration 0.6 g/L, porosity = 0.9321

3 m/hr		5 m/hr		7 m/hr	
Time (min)	C/C_0	Time (min)	C/C_0	Time (min)	C/C_0
71	0.05	-	-	-	-
72	0.05	-	-	-	-
73	0.05	-	-	-	-
74	0.05	-	-	-	-
75	0.05	-	-	-	-
76	0.05	-	-	-	-
77	0.06	-	-	-	-
78	0.06	-	-	-	-
79	0.07	-	-	-	-
80	0.06	-	-	-	-
81	0.06	-	-	-	-
82	0.07	-	-	-	-
83	0.07	-	-	-	-
84	0.07	-	-	-	-
85	0.08	-	-	-	-
86	0.08	-	-	-	-
87	0.08	-	-	-	-
88	0.08	-	-	-	-
89	0.09	-	-	-	-
90	0.09	-	-	-	-
91	0.09	-	-	-	-
92	0.10	-	-	-	-
93	0.11	-	-	-	-
94	0.12	-	-	-	-
95	0.12	-	-	-	-
96	0.13	-	-	-	-
97	0.14	-	-	-	-
98	0.15	-	-	-	-
99	0.17	-	-	-	-
100	0.19	-	-	-	-
101	0.21	-	-	-	-
102	0.21	-	-	-	-
103	0.22	-	-	-	-

Table E-2 (continued): Breakthrough data of variation flow rate at modified stainless

filter, particle concentration 0.6 g/L, porosity = 0.9321

3 m/hr		5 m/hr		7 m/hr	
Time (min)	C/C_0	Time (min)	C/C_0	Time (min)	C/C_0
104	0.23	-	-	-	-
105	0.23	-	-	-	-
106	0.24	-	-	-	-
107	0.25	-	-	-	-
108	0.27	-	-	-	-
109	0.27	-	-	-	-
110	0.29	-	-	-	-
111	0.31	-	-	-	-
112	0.33	-	-	-	-
113	0.36	-	-	-	-
114	0.39	-	-	-	-
115	0.43	-	-	-	-
116	0.45	-	-	-	-
117	0.48	-	-	-	-
118	0.52	-	-	-	-
119	0.53	-	-	-	-
120	0.57	-	-	-	-
121	0.59	-	-	-	-
122	0.64	-	-	-	-
123	0.67	-	-	-	-
124	0.70	-	-	-	-
125	0.75	-	-	-	-
126	0.79	-	-	-	-
127	0.79	-	-	-	-
128	0.82	-	-	-	-
129	0.84	-	-	-	-
130	0.87	-	-	-	-
131	0.89	-	-	-	-
132	0.92	-	-	-	-
133	0.93	-	-	-	-
134	0.94	-	-	-	-
135	0.96	-	-	-	-
136	0.97	-	-	-	-
137	0.98	-	-	-	-

Table E-2 (continued): Breakthrough data of variation flow rate at modified stainless filter, particle concentration 0.6 g/L, porosity = 0.9321

3 m/hr		5 m/hr		7 m/hr	
Time (min)	C/C_0	Time (min)	C/C_0	Time (min)	C/C_0
138	0.98	-	-	-	-
139	0.99	-	-	-	-
140	1.00	-	-	-	-
141	1.01	-	-	-	-
142	1.01	-	-	-	-
143	1.02	-	-	-	-
144	1.03	-	-	-	-
Stop		-	-	-	-

Table E-3: Breakthrough data of variation particle concentration at modified stainless

filter, flow rate 5 m/hr, porosity = 0.9321

0.3 g/L		0.6 g/L		1 g/L	
Volume (mL)	C/C_0	Volume (mL)	C/C_0	Volume (mL)	C/C_0
25	0	25	0	25	0
50	0	50	0	50	0
75	0	75	0	75	0.01
100	0	100	0	100	0.02
125	0	125	0	125	0.03
150	0	150	0.01	150	0.05
175	0	175	0.01	175	0.07
200	0.01	200	0.02	200	0.09
225	0.01	225	0.03	225	0.13
250	0.02	250	0.05	250	0.15
275	0.03	275	0.08	275	0.26
300	0.02	300	0.11	300	0.33
325	0.04	325	0.15	325	0.49
350	0.04	350	0.23	350	0.6
375	0.04	375	0.28	375	0.73
400	0.06	400	0.35	400	0.86
425	0.06	425	0.4	425	0.95
450	0.08	450	0.49	450	1.01
475	0.08	475	0.57	475	1.03
500	0.10	500	0.64	500	1.03
525	0.13	525	0.69	525	1.04
550	0.18	550	0.77	550	1.04
575	0.23	575	0.84	Stop	
600	0.28	600	0.86	-	-
625	0.35	625	0.94	-	-
650	0.42	650	0.96	-	-
675	0.47	675	0.98	-	-
700	0.52	700	1.00	-	-
725	0.58	725	1.01	-	-
750	0.63	750	1.03	-	-
775	0.70	775	1.03	-	-
800	0.75	800	1.04	-	-
825	0.80	Stop		-	-
850	0.83	-	-	-	-
875	0.87	-	-	-	-
900	0.91	-	-	-	-
925	0.95	-	-	-	-

Table E-3 (continued): Breakthrough data of variation particle concentration at modified stainless filter, flow rate 5 m/hr, porosity = 0.9321

0.3 g/L		0.6 g/L		1 g/L	
Volume (mL)	C/C_0	Volume (mL)	C/C_0	Volume (mL)	C/C_0
950	0.98	-	-	-	-
975	1.00	-	-	-	-
1000	1.01	-	-	-	-
Stop		-	-	-	-

VITA

Name: Jidanan Kaosaiphun

Date of Birth: September 16, 1989

Place of birth: Saraburi province

Nationality: Thai

University education: 2008-2011 Bachelor's Degree, Department of Chemistry Science, Faculty of Science, Chulalongkorn University, Bangkok, Thailand

Presentation: Jidanan Kaosaiphun, Patiparn Punyapalakul, and Aunnop Wongrueng. Application of Functionalized Superparamagnetic Porous Silicates Adsorbents on Clofibric acid Removal in Wastewater. Annual Conference on Engineering & Information Technology (ACEAIT), 2014, Tokyo, Japan, March 28-30.Organized by Higher Education Forum, Taipei, Taiwan.